Ecosystem Analysis of Phosphorus Impacts and Altered Hydrology in the Everglades: A Landscape Modeling Approach

Fitz, H.C and F.H. Sklar. 1999. pp. 585-620 *In*: Reddy, K.R., G.A. O'Connor, and C.L. Schelske, (Editors). *Phosphorus Biogeochemistry in Subtropical Ecosystems.* Lewis Publishers, Boca Raton, FL, USA

Abstract

The Everglades have undergone significant change in response to altered hydrology and water quality, which is why natural resource managers are now evaluating alternative water and nutrient management strategies for the region. Simulation models are an integral part of the process of understanding complex ecological systems, providing a means to evaluate potential ecosystem response to changes in management. To evaluate various management alternatives on the Everglades ecosystems, we developed a spatially explicit ecosystem model for Water Conservation Area 2A (the Conservation Area Landscape Model, or CALM). The CALM simulates interactions among hydrology, chemistry, and biology of the marsh systems across the landscape, synthesizing ecosystem behavior in response to changing environmental inputs. Calibration results for 1980-1996 indicated good hydrologic and ecological agreement with observed data. Observed and simulated water stage were well correlated ($R^2 = 0.70$). North-south gradients of simulated dissolved inorganic phosphorus in the surface waters (50 - 4 μg P L^{-1}) and in the pore waters (950 - 10 μg P L^{-1}) were spatially and temporally realistic. Likewise, simulated and observed data along the gradient had similar values of peat accretion (5.5 - 3.1 mm yr^{-1}, respectively), macrophyte biomass (1100 - 300 g C m^{-2}, respectively), calcareous periphyton biomass (0 - 52 g C m^{-2}, respectively), and community shifts in periphyton and macrophytes. The model captures the feedbacks among plants, hydrology, and biogeochemistry through process-based algorithms, including the influence of spatial patterns on these processes. For example, in a 17-yr (1980-96) simulation sensitivity analysis of increased evaporative losses, there were more pronounced regions of increased soil P remineralization associated with reduced hydroperiods, which in turn increased macrophyte growth. If future management of the area lowers water levels below those that occurred in the 1980s, the simulation under drier conditions indicates that changes in the system's biogeochemistry are likely to occur beyond those directly linked to reduced allochthonous nutrient loads. In another simulation scenario in which external phosphorus loads

were reduced, the CALM indicated that some landscape measures - such as sorbed phosphorus and macrophyte biomass - would not be immediately affected (improved) in all currently-impacted areas. That scenario indicated that internal cycling of phosphorus would likely continue to maintain a eutrophic state in some impacted areas for years, with soil porewater P increasing for a decade, albeit at reduced rates compared to a simulation with actual, observed loads. In that reduced-load scenario run, appearance of calcareous periphyton within the currently-impacted zone reflected the reduction in surface water nutrients compared to the nominal run. However, macrophyte biomass (and thus shading) was not greatly reduced in much of that zone, thus preventing calcareous periphyton from attaining high densities that are found in pristine areas. We are currently working on refinements and further model verification in anticipation of applying the model framework towards evaluating Everglades restoration alternatives in the entire Everglades/Big Cypress region.

KEYWORDS: Everglades, ecosystem, landscape, simulation model, wetland, biogeochemistry, hydrology, plant biology, water management.

Introduction

During the early decades of the 20th century, large regions of south Florida were drained by construction of canals. In 1948 the US Army Corps of Engineers (USACOE) initiated the Central and South Florida (C&SF) Project Study, an extensive engineering project which ultimately led to the compartmentalization of large regions of the Everglades. These impounded Water Conservation Areas (WCAs) are now part of a network of some 2500 km of canals and levees that provide flood control and water supply for the urban and agricultural sectors of south Florida, with about one half of the original Everglades converted to agricultural and urban land uses. However, with recognition that the natural system of the region has been impacted by these engineering works, the USACOE, authorized by the US House of Representatives and Section 309(1) of the Water Resources Development Act of 1992, has implemented a “Restudy” of the management network with the primary goal of restoring the remnant Everglades back towards historical attributes while still providing adequate water supply and flood control. A large part of this effort involves restoring historical water depths and hydroperiods in the WCAs and Everglades National Park (ENP). Critical to successful Everglades restoration are evaluations of the water quality and biology associated with Restudy flow patterns and sources.

Many of the Restudy evaluations use models to analyze possible results of Everglades restoration scenarios. One of the principal tools used in evaluation of alternate management scenarios is the South Florida Water Management Model (SFWMM) (MacVicar et al. 1984, HSM

1997), a grid-based hydrologic model that simulates regional water management. A companion model to the SFWMM is the Natural System Model (NSM) (Fennema et al. 1994, Bales et al. 1997), which simulates pre-drainage hydrology in the region by removing all water management engineering works and using best estimates of historical land elevation and vegetation type. One of the fundamental Restudy assumptions is that these models can be used to develop pre-drainage hydrologic targets for Everglades restoration. However, restoration strategies also need to evaluate how the Everglades system will respond to hydrology plus other variables, such as those that are associated with phosphorus (McCormick and O'Dell *in press,* Miao and Sklar *in press,* Rutchey and Vilchek *submitted*), heavy metals (Ogden et al. 1974), and sea level rise (Meeder et al. 1996). Therefore, other models are being developed to furnish a more comprehensive analysis of ecosystem change due to restoration activities. For example, the Everglades Water Quality Model (EWQM) (Chen et al. 1997), using output from the SFWMM, applies statistically derived, first-order settling rates of total phosphorus to determine transport of phosphorus through the Everglades. Another modeling tool is a tracking model (Walker 1998) that employs regression analyses of observed data to predict total phosphorus at various water control structures in the Everglades.

An important distinction between the above models and the more process-oriented model we present is the extent to which underlying mechanisms of ecosystem dynamics are explicitly incorporated. The process-oriented model may have statistically derived parameters in its equations. However, the model structure incorporates dynamic feedbacks among the variables and it responds effectively to a broad range of inputs and conditions. A purely statistical model should not be used to predict the response of a dependent variable when the independent variable goes outside the range of observed values used to construct the model. A process-based ecological model can characterize ecosystem dynamics under a wide variety of conditions, using known characteristics associated with the processes such as nutrient uptake and remineralization.

The importance of dynamic interaction is further accentuated when spatial heterogeneity of the model space is considered. Spatially explicit process-based models account for this heterogeneity. The pattern of these processes is a function of the connectivity of different subregions and the exchange of matter or information among them. As spatial patterns change, they alter flow of material and information and thus influence local processes. Conversely, changing processes alter ecosystem characteristics within a region and thus alter its spatial pattern. It is the confluence of spatial patterns and system processes that is our focus of ecological modeling of the Everglades. We present here a process-based, spatially explicit ecological model framework in order to understand the long term, large-scale consequences of management changes. The Everglades Landscape Model (ELM), designed to evaluate the ecosystem responses

to modified water and nutrient management policies (Fitz et al. 1993), is the framework for this paper. The ELM covers most of the natural system of the Everglades and Big Cypress region and incorporates the direct and indirect interactions associated with hydrology, phosphorus cycling, detrital decomposition, primary production, and habitat succession. In this manuscript, we present results of a rescaled ELM that was applied to Water Conservation Area 2A (WCA-2A) in the northern Everglades. WCA-2A has well-documented ecological gradients (Koch and Reddy 1992, Jensen et al. 1995, McCormick and O'Dell *in press,* McCormick et al. *in press-a,* Miao and Sklar *in press*) in response to altered nutrient and water flows associated with water and agricultural management in the Everglades Agricultural Area (EAA). This rescaled ELM is called the Conservation Area Landscape Model (CALM), and it was developed to: 1) address questions concerning the processes underlying specific landscape changes in WCA-2A; and 2) calibrate and debug the ELM code in an area with significantly fewer vegetation types and less water management engineering complexity compared to the entire Everglades/Big Cypress region. We will discuss the characteristics of WCA-2A, the CALM structure, its calibration, and ecosystem properties that emerge from CALM simulation sensitivity analyses.

Landscape characteristics

Water management

In the northern Everglades, WCA-2A is a 433 km^2 wetland that was impounded in its present form in 1961 (Figure 1). The Everglades Agricultural Area (EAA) is on its northwest boundary, with urban development along its eastern boundary. Entirely surrounded by levee systems with water control structures along its perimeter, WCA-2A has undergone a number of operational changes during its history (Light and Dineen 1994). WCA-2A water stage has been regulated for various combinations of water storage (relatively deep inundation) and environmental protection (lower, varying stages) of the marshes and tree islands in the area.

Major water discharges into WCA-2A are along the L-39 levee through the S-10 A, C, & D gated spillways (Figure 1), each of which have a design discharge capacity of 132 $m^3\ s^{-1}$ (Cooper and Roy 1991). This water enters an interior borrow canal that extends along portions of levees of the northeast and eastern WCA-2A borders, respectively, exchanging water with the adjacent interior marshes. The S-10E inflow structure at the northern tip of L-39 is relatively small in capacity, with a design discharge capacity of 12 $m^3\ s^{-1}$. Another major inflow is via S-7 (70 $m^3\ s^{-1}$ capacity) at the western tip of the WCA, where water enters the North New River Canal along the WCA interior and exchanges with the surrounding marshes. Major discharges from the WCA are via the three S-11 structures (each with 158 $m^3\ s^{-1}$ capacity) from the North New River Canal in the

southwest, with comparatively minor discharge volumes from an interior borrow canal along the southeastern levee via S-143 (14 m^3 s^{-1} capacity), S-144, 145, & 146 (each with 6 m^3 s^{-1} capacity), and S-38 (14 m^3 s^{-1} capacity).

Water flow through these structures has varied dramatically within and among years. Seasonal and interannual changes in rainfall intensity alter the inflows to the WCA, water management regulation schedules have varied over the years, and deviations from those targets occurred based on overriding water supply and flood control needs elsewhere. Interannual variations in structure discharges are large, with a pattern that generally follows the trends in annual rainfall (Figure 2).

Rainfall

South Florida rainfall is generally described as having a wet season from June through September and a dry season during the remainder of the water year. Annual rainfall sums for WCA-2A (measured at S-7) averaged 132 cm yr^{-1} between (calendar years) 1965 - 1996 (Figure 2), ranging from 107 to 210 cm yr^{-1}. During several years in the mid-1990s there were extreme flood conditions due to very heavy rains. The late 1960s and early 1980s also were conspicuous for unusually high rainfall periods. Droughts of varying magnitudes occurred on a number of occasions during this record.

Nutrient loading

External nutrient loads to WCA-2A come from several sources: wet and dry atmospheric deposition, the S-10 structures, and the S-7 structure. The S-10A, C, D, and E structures receive water and dissolved/suspended nutrient constituents from the Hillsboro Canal along the southern portion of WCA1, whose principal source is the S-6 structure discharging from the EAA. In general, the highest P loads from the Hillsboro Canal into WCA-2A have been from S-10D (Figure 3a), with decreases downstream at S-10 C followed by S-10A. The most upstream S-10E structure has high nutrient concentrations, but loads are low relative to S-10D due to S-10E‘s lower volume capacity and operational rules. EAA discharges through S-7 in the west is the other significant contributor to the WCA-2A P loads.

Annual load from atmospheric sources is uncertain due to the difficulties in measuring wet and dry deposition. For the CALM, we assumed a constant median (reducing bias from possible contamination due to birds and insects) of 0.010 mg L^{-1} dissolved inorganic P in rainfall based on a 2 year period from collectors managed by the South Florida Water Management District. This equals a mean wet deposition rate on the order of 20 mg P m^{-2} yr^{-1} between 1978 - 1996. There are few available dry deposition measurements, but several sources at a conference on atmospheric

deposition in south Florida (SFWMD 1997) indicate that the rate may be approximately half that of wet deposition in the vicinity of WCA-2A. Thus, we assumed a total median atmospheric deposition on the order of 30 mg P m^{-2} yr^{-1} to WCA-2A, or approximately 12.9 Mg (metric ton) P yr^{-1} to the entire WCA. This WCA-wide atmospheric load of 12.9 Mg is only 21% of the 19-year annual average total water control structure and atmospheric P load. Input through the S-7 plus S-10 structures (47.7 Mg P yr^{-1}), compared with atmospheric deposition, has a more localized distribution within WCA-2A.

The largest structure outflows are via the S-11 structures (Figure 3b), which transport water and nutrients from the North New River Canal to WCA-3A. While summed S-11 dissolved inorganic P outflows are similar in magnitude to that of the corresponding S-7 inflow (12.6 and 13.2 Mg P yr^{-1}, respectively), P introduced through the S-10 structures is largely routed through the marshes. During the period of record for nutrient measurements (1978-1996) at the major water control structures, there has been a large, positive net P load to WCA-2A. The temporal distribution of this load exhibited distinct peaks in 1982, 1983, 1988, 1992, and 1994 (Figure 3c), with the peak loads in the 1990's (> 75 Mg P yr^{-1} in 1994) primarily due to very large water flows despite reduced P concentrations.

Topography

Land surface elevation has been surveyed on a relatively fine scale in WCA-2A (Keith and Schnars 1993), and the point data interpolated using the CREATETIN procedure in ARC/INFO (ESRI, 1982-95) to produce a 20 m resolution digital raster map (Figure 1). There is less than 1.5 m difference in elevation over the 30 km distance between the north and south extremes. Sloughs and depressions are apparent throughout the region, including a north-south slough starting south of the S-10C structure. The extreme southern tip and the southeast corner are two locations with very low elevation, while the northern tip has a significant rise in topographic relief. Prior surveys of WCA-2A elevation from which historical changes in elevation could be inferred are unavailable.

Macrophytes and periphyton

WCA-2A is a complex mosaic of habitats such as tree islands, sawgrass (*Cladium*) marshes, spikerush (*Eliocharis*) sloughs, open water, and cattail (*Typha)* marshes (Rutchey and Vilchek 1992), with mixtures, patches, and gradients of these macrophytes throughout the region. Rutchey and Vilchek (1992) found significant areas dominated by *Typha*, which did not appear to be found in abundance within the historical Everglades (Davis 1943). Whereas satellite image classification techniques were employed to estimate changes in *Typha* distribution between 1973

and 1991 (Jensen et al. 1995), more accurate recent photo-interpretations (Rutchey and Vilchek *submitted*) found a 70% increase in cattail coverage in WCA-2A between 1991 and 1995.

WCA-2A chemical and biological gradient

As evidenced by the changes in *Typha* distribution, a number of biogeochemical characteristics have significantly changed in the region south of the S-10 structures. Downstream gradients of soil nutrients, surface water nutrients, periphyton, and macrophyte community structure along a ~10 km distance have been well documented (Swift 1984, Swift and Nicholas 1987, Koch and Reddy 1992, Urban et al. 1993, Jensen et al. 1995, McCormick and O'Dell *in press,* McCormick et al. *in press-a,* Miao and Sklar *in press*). The causal mechanisms for these biological and chemical gradients have been the focus of extensive research and debate in south Florida. Reddy et al. (1991) measured the spatial distribution of a variety of biogeochemical variables and accumulation rates, and found that soil nutrient concentrations at the S-10 structures were an order of magnitude higher than reference sites in the center of WCA-2A. Koch-Rose et al. (1994) provided evidence that microbial activity and P remineralization were P-limited in pristine areas of WCA-2A. McCormick and Scinto (1998) found a periphyton community shift downstream of the S-10 structures where total (organic and inorganic) phosphorus (TP) concentrations dropped below 12 $\mu g\ L^{-1}$. Miao and Sklar (*in press*) found physiological differences between cattail populations immediately downstream of the S-10 structures and those at interior reference sites. Richardson et al. (1995) determined the response of a variety of biological indicators to changes in phosphorus and hydroperiod in WCA-2A. The ELM framework was used to synthesize this type of gradient information for calibration and validation of the CALM.

Model characteristics

Objectives

The Everglades Landscape Model (ELM) was designed to be a regional landscape simulation model to address the effects of different management scenarios on the ecosystems in the entire Everglades. The Conservation Area Landscape Model (CALM) was an implementation of the same code applied to a smaller, simpler region. This application was used to evaluate and calibrate some of the model's ecological dynamics within the intensively studied landscape of WCA-2A. The ELM and CALM are intended to provide a tool to:

1) estimate the water demands of the Everglades in terms of adequacy of water flow and water levels to achieve user-defined landscape/ecosystem characteristics;

2) predict vegetation changes that result from specific hydrology and associated water quality regimes, simulating the inter-relationships among water quality, hydrology, and vegetation, and the influence of these relationships on habitat quality; and

3) provide a focus to research programs and models on other scales.

General structure

The CALM simulates interactions among fundamental ecological processes (Figure 4), with the objective of quantifying the response of vegetation. Simulations can be several decades in duration, or as many as 50 years depending on the available information. Growth of macrophyte and periphyton communities responds to available nutrients, water, sunlight and temperature. Hydrology in the model responds directly in turn to the vegetation via linkages such as Manning's roughness coefficient and transpiration losses (Fitz et al. 1993). Phosphorus and nitrogen cycles include uptake, remineralization, sorption, diffusion, and organic soil loss/gain. The magnitude and duration of nutrient availability and water depths alters habitat patterns via a habitat transition algorithm.

Central to the CALM structure is division of the landscape into square grid cells to represent the landscape in digital form. Superimposed on this grid network are canal/levee vectors along the boundaries of the region. Within this spatial structure are four fundamental components of the simulation:

1) The "unit" model (Fitz et al. 1996): This is the most basic building block of the model, simulating the temporal dynamics of important biological and physical processes within a grid-cell. Different vegetative habitats have unique parameter values, but all habitats run the same unit model;

2) The management component: Canals and associated levees are represented by a set of vector objects that interact with a specific set of raster landscape cells (Fitz et al. 1993, Voinov et al. *submitted*). This allows for rapid flux of water and dissolved nutrients over long distances.

3) The Spatial Modeling Environment (Maxwell and Costanza 1995): This provides for the translation of the unit model into a spatially explicit framework, integrates all of the spatial and non-spatial fluxes, and coordinates input/output.

4) The data component: Spatially explicit data such as habitat type, elevation, and canal vectors are maintained in GIS layers, and other databases store time series inputs (e.g., rainfall) and parameters that vary with habitat (e.g., growth rates). The data structure organizes the information and alleviates the need to recompile the model code when evaluating the effects of different management scenarios.

The resulting spatially explicit model (Figure 5) contains a unit model that calculates within-cell dynamics depending on each cell's parameter set, with the interactions among cells via hydrologic fluxes propagating state changes across a heterogeneous space. It is this simulation of the influence of the landscape heterogeneity on ecosystem (cell) processes, and the concomitant influence of the ecosystem (cell) processes on shaping local pattern, that allows such spatially explicit process models to explore ecosystem properties at relatively large scales.

Scales and boundary conditions

The CALM boundaries encompass the entire 433 km^2 wetland within the levees that define WCA-2A. We used 1,734 cells of 0.25 km^2 fixed grid size and assumed that each individual cell is homogenous in all of its characteristics. The model was run with a 1 hr time step for all horizontal flows of water and dissolved nutrients. All other flux calculations were made at a 12 hr time step. Boundary conditions for water and nutrient inflows and outflows were associated with the atmosphere and water management along the WCA's levees. Daily rainfall measured at the S-7 structure (Figure 1) was applied to all model cells. As described earlier, dry deposition was not explicitly simulated. Atmospheric deposition was assumed to have a constant concentration of 0.015 mg P L^{-1}. The total deposition using these rainfall-driven inputs averaged approximately 30 mg P m^{-2} yr^{-1}.

Daily observed measurements of water volume and associated P concentration were applied to the S-7, S-10A, S-10C, S-10D, and S-10E inflow water control structures. Because nutrient concentrations were measured at a minimum of bi-weekly intervals, we used a linear interpolation across dates with missing values (Walker 1998). For outflow of nutrients, observed measurements of water outflows through S-11A, S-11B, and S-11C were multiplied by nutrient concentrations in adjacent donor cells/canals from the simulation. Outflows through the S-38, S-143-146 structures were driven by management rules, in which the targeted stage was compared at each time step with simulated stage at the 2-17 gage (see Figure 1). Regulatory water (and nutrient) releases were applied through these structures when the stage was greater than the target. Seepage across boundary levees was calculated using a fixed hydraulic head in the borrow canals bordering WCA-2A.

Process simulation

Feedbacks among physical, geochemical, and biological components of a system have long been recognized to be critical in determining ecosystem properties. Due to the nature of the myriad interactions within the Everglades and the CALM, processes that have an influence on, and are affected by, phosphorus can virtually include every ecosystem component. The CALM does not

attempt to simulate them all. Here we present a summary of the model structure and provide details of some of the modules and equations that most directly relate to transport and fate of phosphorus. Other details of all state variables, algorithms, and equations are published elsewhere (Fitz et al. 1996).

Hydrology -- The CALM hydrology module simulates ponded surface water, water in unsaturated soil, and saturated water below the water table, coupling the surface and ground water components. Fluxes among those variables (Figure 6) involve rainfall, evaporation, infiltration, percolation, saturated/unsaturated transpiration, and horizontal movement of surface and saturated water. Many of the hydrologic algorithms are based on those developed for the SFWMM (MacVicar et al. 1984, HSM 1997). Differences are associated with accommodating fine-scales and direct linkages with vegetation. Evaporation and transpiration in CALM are driven by the calculated air saturation deficit, leaf area exposed above any ponded surface water, and canopy morphology (Fitz et al. 1996), in relation to a simple evaporative model (Christiansen 1968). Transpiration losses further depend upon the availability of water relative to the root zone depth. As will be indicated in the model results section, transpiration in a flooded wetland can transport P as a result of the associated surface to soil porewater advective flux of water and dissolved constituents.

Horizontal transport of water and nutrients is a fundamental component of the water quality component of the model. Flows of water among grid cells were calculated using a mass balance, finite difference algorithm solving two dimensional horizontal diffusion equations. We used an alternating direction, explicit method to solve the Manning's equation for overland flow, which for equal, square grid cells can be discretized into:

$$Q = \frac{h^{\frac{5}{3}} L^{\frac{1}{2}} \Delta H^{\frac{1}{2}}}{n} \qquad (1)$$

where Q is the volumetric flow velocity ($m^3\ d^{-1}$), h is the water depth (= hydraulic radius, m) above ground elevation in the source cell, L is the length of a grid cell (m), ΔH is the difference (m) in water stage between the source and destination cells, and n is the empirically-derived Manning's roughness coefficient. The equation was constrained such that the volume flux could not result in a reversal of the sign of the ΔH within any iteration of a cell-cell flux. A four-way, alternating direction algorithm (Voinov et al. *in press*) was used to solve this flow velocity equation. The Manning's n value was a function of the dynamic height of the particular vegetation type relative to water depth (Fitz et al. 1996) according to:

$$n = n_{\max} - \left| (n_{\max} - n_{\min}) \left(2^{(1 - h/mac)} - 1 \right) \right| \quad (2)$$

where n_{min} and n_{max} are the respective minimum and maximum roughness coefficients associated with a cell's macrophyte/soil characteristics, and *mac* is the macrophyte height.

The water management system associated with WCA-2A, while not as extensive and complex as found within the larger ELM region, has significant impact on water distribution in WCA-2A. We developed a technique to dynamically exchange water among the canal vectors and the raster grid cells such that the vectors overlaid cells in their true orientation and maintained the correct area of interaction among the two object types (Fitz et al. 1993, Voinov et al. *submitted*). The water management module provided for: a) flow of water and nutrients along canals; b) exchange of water and nutrients among grid cells and canal vectors via overland or groundwater flow; and c) controlled flow of water and nutrients among canals and/or cells via water control structures.

Canal reaches were defined by a series of points defining their exact location. A geometry algorithm determined the length and type (overland vs. seepage) of each segment's cell interaction using a technique that can be generalized to other raster and vector objects for simulation (Voinov et al. *submitted*). Water and nutrients were distributed along the length of a canal, with exchanges through control structures and among cells and canal reaches. Stages in the canals and in all of the interacting cells were updated using an iterative relaxation routine (used in the SFWMM, (HSM 1997)) to equilibrate the water levels until converging to a minimum error. All flow calculations contained constraints to ensure mass balance. When the Manning's equation (1) was applied to overland flows between a canal and a cell, the hydraulic radius was that of the canal (hr_{can}) if flux was from the canal into a cell, or that of the cell (hr_{cell}) if flow was from the cell into the canal:

$$hr_{can} = \frac{l_{can} w_{can} d_{can}}{A_{cell}}, \qquad hr_{cell} = \frac{(A_{cell} - l_{can} w_{can}) h}{A_{cell}} \quad (3)$$

where l_{can} is the canal length (m), w_{can} is the canal width (m), d_{can} is the canal depth (m), A_{cell} is the area of the cell (m^2). While the algorithm allows levees to be absent, on both sides of a canal reach, or on either side, the latter was the only case needed in the CALM. Because we used fixed external stages for boundary conditions, seepage flows across levees and subsurface groundwater flows exiting the system depended only on changing water stage within WCA-2A. This

simplification was justified under the assumption that water management generally targets a maximum stage in the urban and agricultural areas adjacent to WCA-2A.

The WCA-2A stage regulation targets determined whether the S-143-146 and S-38 structures (Figure 1) were open to release water out of the WCA, the rate of which was calculated using a simplified weir flow equation:

$$Q_{out} = Q\left(h_{can} - h_{ext}\right)^{1.5} \quad (4)$$

where Q_{out} is the calculated flow through the structure ($m^3\ d^{-1}$), Q is the weir flow rate coefficient using a common 10 m weir length, and h_{ext} is the fixed external water stage height (m). Structures (S-7, S-10's, and S-11's) driven by observed fluxes had all flows determined by the time series data.

Biogeochemistry -- The principal components of the P biogeochemical dynamics included: a) P storage in suspended organic matter (*SOM*), accreted organic matter (*AOM*) in soils, standing dead detritus (*SDD*), macrophytes, periphyton, and consumers; b) remineralization of *SOM* and *AOM* into inorganic *P* dissolved in surface and soil water; c) reversible sorption of *P* to soils; d) uptake of soil and surface water inorganic *P* by macrophytes and periphyton, respectively; and e) horizontal (among cells and canals) and vertical (within-cell) flows of *P* dissolved in water (Fitz et al. 1996). (A similar nitrogen module exists but was not fully implemented for this version of CALM). To facilitate calibration, the live organic matter (macrophytes, periphyton, and consumers) and *SDD* stocks were expressed in organic carbon units (kg C m^{-2}), and the AOM and SOM stocks were expressed in ash free dry mass (kg OM m^{-2}, kg OM m^{-3}, respectively). The P storage in these stocks was determined by fixed, habitat-specific P:C (and C:OM) ratios; the exception was that of the soil *AOM*, which had variable P:C stoichiometry for mass balance accounting.

Organic carbon from mortality of photosynthetic and non-photosynthetic stocks of macrophytes was partitioned between the *AOM* and *SDD* stocks, according to the macrophyte type. *AOM* dynamics were:

$$AOM_t = AOM_{(t-dt)} + \left(AOM_{set} - AOM_{dec}\right)\ dt \quad (5)$$

where, AOM_t and $AOM_{(t\text{-}dt)}$ are the mass densities of accreted organic matter (kg OM m^{-2}) at time t and (t-1), AOM_{set} is the additive ("settling") input from the macrophyte, periphyton, consumer, *SDD*, and *SOM* organic stocks (kg OM $m^{-2}\ d^{-1}$), and AOM_{dec}, is the loss due to decomposition (kg OM $m^{-2}\ d^{-1}$).

Implicit microbial decomposition of the *AOM* carbon stocks was controlled by temperature, available nutrients, moisture availability, and a classification of aerobic vs. anaerobic conditions as shown in the following equations. This AOM decomposition was described by:

$$AOM_{dec} = AOM \left[k_{ar} T_{cf} P_{cf} \left(Usat_{cf} \frac{H_{ar}}{H_{AOM}} + k_{an} \frac{H_{an}}{H_{AOM}} \right) \right] \quad (6)$$

where k_{ar} is the maximum specific rate of aerobic decomposition (d^{-1}), k_{an} is the modifier for anaerobic decomposition, $Usat_{cf}$ is the proportion (0-1) of soil moisture in the unsaturated zone, and T_{cf} is the 0-1, dimensionless temperature control function (Lassiter 1975):

$$T_{cf} = e^{0.2\left(T - T_{opt}\right)} \left(\frac{T_{max} - T}{T_{max} - T_{opt}} \right)^{0.2\left(T_{max} - T_{opt}\right)} \quad (7)$$

where T is the soil water temperature, T_{max} is the maximum temperature of acclimation (˚C), and $_{Topt}$ is the optimal temperature at which the decomposition rate is maximal (˚C). P_{cf} is the available phosphorus control function (dimensionless, 0 - 1), in the form of:

$$P_{cf} = \frac{P_{pwat}}{\left(P_{pwat} + K_{AOM}\right)} \frac{PC_{AOM}}{\left(PC_{AOM} + PC_{ref}\right)} \quad (8)$$

where, K_{AOM} is the half saturation coefficient (mg P L^{-1}) for microbial uptake, P_{pwat} is the concentration of P in the soil pore water, PC_{AOM} is the P:C ratio of the *AOM*, and PC_{ref} is the reference P:C ratio for that habitat type (Reddy et al. 1991). H_{ar} and H_{an} were the thickness (m) of the aerobic and anaerobic soil zones, respectively:

$$\begin{aligned} H_{ar} &= \min\left(H_{us} + H_{tar}, H_{AOM}\right), \\ H_{an} &= H_{AOM} - H_{ar} \end{aligned} \quad (9)$$

where, H_{us} is the variable height of the unsaturated water zone (m), H_{tar} is the fixed height (m) of the thin aerobic layer for each habitat type in the model, and H_{AOM} is the fixed height (m) of the active *AOM* layer for each habitat type. No plant uptake or microbial dynamics were considered below this (30-50 cm) active layer.

Phosphorus and organic carbon from periphyton mortality were routed into the SOM compartment at the same P:C ratio as live periphyton. Decomposition of *SOM* followed the same general form as that of *AOM* (Equation 6), except we assumed only aerobic conditions and fixed stoichiometry. Similarly, the *SDD* stock assumed the same P:C ratio as its macrophyte source.

Losses of *SOM* and *AOM* phosphorus from carbon decomposition were determined through the respective *SOM* and *AOM* P:C stoichiometry. The P:C ratio of *AOM* was calculated from the *AOM* carbon and *AOM* phosphorus (*AOM_P*, kg m^{-2}) variables. *AOM_P* dynamics were determined by:

$$AOM\_P_t = AOM\_P_{(t-1)} + \left(AOM\_P_{set} - AOM\_P_{dec}\right)\ dt \tag{10}$$

where, AOM_P_t and $AOM\_P_{(t-1)}$ are *AOM_P* at time t and (t-1), respectively, AOM_P_{set} is the "settling" input associated with the source (fixed stoichiometry) AOM_{set} , and AOM_P_{dec} is the P loss associated with the AOM_{dec} decomposition such that:

$$AOM\_P_{dec} = AOM_{dec} PC_{AOM} \max\left(1 - \frac{PC_{ref}}{PC_{AOM}}, 0\right) \tag{11}$$

where, PC_{AOM} converges to PC_{ref} as new organic matter decomposes.

In addition to total P storages associated with AOM in soil, we considered the dynamics of labile inorganic P that is loosely sorbed to the soils in the active AOM layer (*P_sorb*). The active *AOM* layer of the soils in the model was assumed to be homogeneous in vertical profile, with a fixed porosity and no change in the P:C ratio or *P_sorb* with depth. We used a modified Freundlich adsorption model (Richardson and Vaithiyanathan 1995), accounting for antecedent phosphate sorbed to the soils:

$$P\_sorb(t) = P\_sorb(t - 1) + \left(k_{sb} P_{pwat}^{\ 0.8} - P\_sorb(t - 1)\right) dt \tag{12}$$

where, k_{sb} is the adsorption coefficient (L kg^{-1}), and P_{pwat} is the *P* concentration in the soil pore water (mg L^{-1}). Using data from (Richardson and Vaithiyanathan 1995), k_{sb} varied linearly with P_{pwat} within the observed range of Everglades soil pore water concentrations.

Biology -- Growth of macrophytes and periphyton was influenced by available nutrients, light, water, temperature, and density dependence. While these relations are described in Fitz *et al.* (1996), below we describe some of the details related to P uptake by plants and algae. Plant growth via carbon fixation was responsible for the removal of *P* from the soil or surface water. This removal was based upon a fixed stoichiometric (P:C) ratio for each habitat type. Growth was limited by inorganic P according to Monod kinetics:

$$MAC\_P_{cf} = \frac{P_{pwat}}{\left(P_{pwat} + MAC\_K_s\right)} \tag{13}$$

where MAC_P_{cf} is the dimensionless P-limiting function for macrophytes, and MAC_K_s is the half saturation coefficient (mg P L^{-1}) for macrophyte uptake. The same relationship, parameterized with a K_s value and compared to P in surface water, was used to constrain growth of non-calcareous periphyton communities. Calcareous periphyton, most abundant in unenriched regions of lower phosphorus, rapidly ceased growth as an upper surface water P concentration (McCormick et al. *in press-a*) was approached:

$$CPer\_P_{cf} = \frac{P_{swat}}{\left(P_{swat} + K_{CPer}\right)} \min\left(\frac{ThrP_{CPer} - min\left(P_{swat}, ThrP_{CPer}\right)}{ThrP_{CPer} - K_{CPer}}, 1\right) \quad (14)$$

where $CPer\_P_{cf}$ is the dimensionless nutrient control function for calcareous periphyton, K_{CPer} is the half saturation coefficient (mg P L^{-1}) for calcareous periphyton uptake, P_{swat} is the P concentration in surface water, and $ThrP_{CPer}$ is the threshold P concentration above which growth ceases.

While shifts in periphyton community type (calcareous vs. non-calcareous) occurred due to their relative growth characteristics in the presence of varying water column P concentrations, macrophyte community shifts were based on the cumulative impacts of both available P and water depth. For each cell we evaluated the number of weeks that contained conditions favorable for each possible habitat type, switching to the new habitat type when conditions merited. Each model cell was evaluated on a daily basis for each of the two conditions for all possible habitat types:

$$\begin{aligned} PLo_i \le P_{pwat} \le PHi_i, \\ HLo_i \le h \le HHi_i \end{aligned} \quad (15)$$

where PLo_i and PHi_i were the respective lower and upper thresholds of porewater P concentrations (P_{pwat}) for the ith habitat type (i=0,1,2, for sawgrass-dominant, cattail-dominant, and cattail-present), and HLo_i and HHi_i were the respective lower and upper thresholds of surface water depth (h) for the ith habitat type. If a cell met either criteria for habitat i, a counter was incremented for that habitat type, regardless of the cell's current habitat type designation. When counters for water depth and for P conditions in a cell exceeded the elapsed (potentially discontinuous) number-of-weeks criteria, the cell's habitat type classification switched to the new type and counters were set to 0.

Model initialization

The CALM was initialized using a series of maps for the conditions expected to have been present in the 1980 landscape. Elevation was aggregated from 20 m to 500 m resolution (Figure 1) using cell averages, and 3 cm was uniformly subtracted to account for soil accretion (Reddy et al.

1993) during the 13 yrs between 1980 and the elevation measurements. The 1982 cattail and sawgrass distribution map (Jensen et al. 1995) was aggregated from 30 m to 500 m resolution using modal frequencies within the model grid cells, with a total of 26 km^2 coverage by cattail and a sawgrass/cattail mixture.

An estimate of the spatial distribution of soil P was made from recent data collected by Reddy et al. (1991). Their 1990 data of total phosphorus in the 10-20 cm soil depth layer was used to estimate the total P in the 0-30 cm soil profile for 1980. This was accomplished with a linear, inverse-weighted nearest neighbor algorithm and the assumption that similar soil equilibrium processes existed in 1980. We also assumed that this 1980 pattern of soil P influenced the initial distribution of macrophyte biomass. A scaling factor based upon the soil P was used to calculate the initial 1980 standing stock of live and dead macrophyte biomass for each vegetation type. Periphyton were initialized to a constant throughout the region. Initial water stage for each cell was developed by running the CALM for one year with a constant "management" target (controlling outflows) that was equal to the observed, January 1980, stage at the 2-17 gage.

Model Results: Calibration

We tested the model over a 17-yr time span (1980 - 1996) that encompassed the hydrologic spectrum ranging from extreme drought years to extremely wet years (Figure 2). Water quality monitoring data at water control structures used to drive the model were generally unavailable before 1980.

Hydrology

A useful summary of hydrologic conditions is the annual hydroperiod, or the number of days during a water year (starting in October) with positive water depths. Hydroperiod patterns (Figure 7) were indicative of the elevation gradients in the ridge and slough regions interspersed through the area and the influence of nearby canal inflows and outflows. Simulated water stage had a substantial degree of concordance with observed stage (m, 1929 NGVD) at the 2-17 gage for the 17 yr simulation period (R^2 = 0.70, RMSE = 0.21 m). As Figure 8 indicates, there was good agreement between simulated and observed data for the majority of the simulation record during both low and high water events. However, several substantial deviations occurred during the later years of the simulation, and in particular during the 1995 drawdown of WCA-2A following an extreme flood year. We feel that because the CALM v1.0 was driven by observed flows through only the major structures (i.e., S-7, S-10, and S-11), these discrepancies are the result of historical managerial deviations from water control structure operational criteria for S-143, S-144, S-145, S-146 and S-38 (which were driven by management rules in the simulation).

Phosphorus

Simulated P dissolved in the interstitial porewater gradually increased in the regions near the S-7 and S-10 structures and produced a spatial pattern by mid-1990 similar to that found by Reddy et al. (1991) and DeBusk et al. (1994) (Figure 9). Mean porewater P concentrations of the simulated and observed data along the transects (Figure 10a) were similar at all but the most eutrophic (F1) sites. The field observations are mean values from a 1.5 yr (August 1995-97) unpublished study (Newman *pers. comm.*) with quarterly samples along the WCA-2A gradient. The simulated and observed P concentrations declined rapidly along the transect to near 0.01 mg L^{-1} in the unimpacted sites. The model overestimated mean porewater P at the enriched F1 site (0.95 ± 0.2 mg L^{-1} vs. 0.5 ± 0.3 mg L^{-1}), but closely simulated the observed data at the enriched F2 site, only 2 km further downstream.

The simulated final concentrations of phosphorus that was sorbed to the peat substrate declined from 81.2 to 3.6 mg kg^{-1} from F1 to U3, respectively, similar to that observed by Richardson and Vaithiyanathan (1995) along three 10 km transects. In that study, the maximum concentration was 95.6 mg kg^{-1} near the canal and the minimum was 1.0 mg kg^{-1} at a distance of 10.5 km downstream.

The P dissolved in surface water likewise demonstrated a realistic gradient along the transects from north to south, with simulated and observed concentrations during a 3 yr period being generally similar (Figure 10b). The field observations are mean values from a 3 yr study (April 1994-96) with biweekly samples along the WCA-2A gradient (McCormick *pers. comm.*). Observed F1 transect data, downstream of S-10D, exhibited numerous excursions of high surface water concentrations and high variance (0.10 ± 0.11 mg L^{-1}) compared to the E1 counterpart (0.05 ± 0.03 mg L^{-1}), downstream of S-10C. This particular dynamic at F1 was not observed in the simulations. In the observed and simulated data, P concentrations declined to near laboratory detection limits (0.004 mg L^{-1}) in the unimpacted sites.

Organic Matter

Soil peat has been estimated to accrete at rates between 0.5 to 0.7 cm yr^{-2} in the vicinity of the enriched F1 site, decreasing to 0.25 cm yr^{-1} near the unenriched U3 site (Craft and Richardson 1993, Reddy et al. 1993). The CALM simulated accretion rates, calculated as the average rate during the 17 yr simulation period, closely matched these estimates (Figure 10c), slightly underestimating the accretion rates in the impacted area.

Observed biomass of *Cladium* and *Typha* communities steadily decreased downstream of the S-10 inflow structures (Miao and Sklar *in press*), and was closely simulated by the CALM

(Figure 10d). Macrophyte biomass ranged from approximately 1.0 kg C m^{-2} at impacted sites where *Typha* was dominant, to 0.3 kg C m^{-2} at unimpacted sites where *Cladium* was dominant. There were no consistent seasonal biomass changes of *Typha* or *Cladium* observed in WCA-2A (Davis 1989) or the simulation. Interannual variations were common during the period, with simulated *Cladium* biomass at the U3 site exhibiting short term (ca. one-season) increases up to densities of 0.5 to 0.6 kg C m^{-2} (e.g., in 1988), in response to combinations of relatively low water levels (Figure 8) and high nutrient loads (Figure 3c). Much of the pattern of the documented (Rutchey and Vilchek *submitted*) spread of *Typha* southward along the transect was captured by the model (Figure 11), with 44 km^2 cattail cover by 1991 (53 km^2 observed) and increasing to 117 km^2 coverage by 1995 (95 km^2 observed). The overestimates of *Typha* in 1995 were due to the simulation's increased occurrence of low density *Typha* mixed with *Cladium* in the ridge and slough regions south of the S-10 structures.

Simulated periphyton communities showed more temporal and spatial heterogeneity than macrophytes, as periphyton respond quickly to changes in water availability (depth) and nutrient concentration (McCormick *pers. comm.*). The CALM produced realistic periphyton responses to water and phosphorus in addition to the longer temporal response to shading by macrophytes. McCormick et al. (*in press-b*) estimated total periphyton biomass in oligotrophic sloughs or sparsely vegetated habitats of WCA-2A to be ~1000 g AFDM m^{-2}, or approximately 150 g (organic) C m^{-2} depending on the ash content and the ratio of carbon to organic matter (Browder 1982) in those values reported by McCormick et al. (*in press-b*). Simulated maxima of 75 g C m^{-2} were underestimates of those observed values because the model underestimates the amount of slough, and thus overestimates macrophyte shading of periphyton. It should be noted that the vegetation mapping techniques used for WCA-2A did not separate sparse sawgrass habitats from slough habitats (Rutchey and Vilchek *submitted*). Figure 12a shows the magnitude and spatial distribution of calcareous periphyton biomass, with the 17-yr mean increasing along the gradient from the eutrophic to oligotrophic areas (F0 - U3). This was a response to both the influence of "excess" P in the surface water near the S-10 inflows (Figure 12b) and simulated macrophyte biomass changes along the gradient (Figure 12c). Much of the heterogeneity in the simulated pattern within the interior region of WCA-2A was due to elevation differences, with habitats along slough ridges that dried out periodically, as reflected by the hydroperiod distribution (Figure 7).

Model Results: Sensitivity experiments

Of the numerous questions that arise when evaluating phosphorus fate and transport in the Everglades system, several relate to the interactions among hydrologic and biogeochemical dynamics in the soils. For example, when the water table drops below the soil surface, the

unsaturated soil zone becomes more aerobic and thus more favorable for peat oxidation. Subsequent rehydration of the area can potentially increase levels of P in the porewaters. Of course, many other factors can control P concentrations such as sorption, plant uptake, and advection between surface and pore waters.

To determine the effects of altered evapotranspiration on the model P dynamics, we increased the potential evapotranspiration within a sensitivity analysis. We considered increased losses by evapotranspiration to be a surrogate for lower managed water levels, effectively altering the water depths in the region without changing the water control structure or atmospheric inflows (and the concomitant change in P loading). Compared to the reference simulation (the nominal case), the test simulation with increased potential evaporation had lower water levels during much of the simulation. In particular, the depth of the unsaturated zone was frequently greater for more prolonged periods. This produced a feedback that increased decomposition and soil remineralization to inorganic P by as much as 1 mg P m^{-2} d^{-1}, resulting in a greater accumulation of porewater phosphorus in particular regions. Figure 13 shows difference (test run minus nominal run) maps of the mean depth of the unsaturated zone during a dry year (1989), along with the corresponding difference in the mean of the remineralization rate. Associated with the drier zones in the central region was increased P release compared to the nominal run, and an increase in macrophyte biomass in response to increased available nutrients during the simulation. In the eutrophic zone near the S-10 inflows, the area was drier in the test run compared to nominal, but there was little change in decomposition rates, which were high in both the nominal and test runs due to high nutrient availability for microbial processes.

Not all of the increased porewater P in the above analysis was necessarily due to increased peat decomposition. In this model, higher transpiration from the macrophytes can advect surface water and its dissolved nutrients into the porewater zone. Davis (1982) showed that more than half of radio-labeled phosphorus introduced into surface water of marsh enclosures moved into the subsurface soils within ten days. With molecular diffusion being a relatively minor flux, this is indicative that downward advection of surface water appears to be a likely flow pathway for this phosphorus. Water losses by transpiration from the saturated zone are replaced by downflow of ponded surface water (Figure 6), along with any constituents dissolved in that water. How significant is this process in making P available to the root zone? To answer this question, we can conduct a simulation sensitivity analysis to investigate the effects of a difference between a densely vegetated and a sparsely vegetated region. We adjusted the leaf area index of sawgrass and cattail and we introduced a conservative tracer into the flows from the S-10 and S-7 control structures (Table 1). Because the model's total evapotranspiration (ET) is apportioned between evaporation and plant transpiration, we can qualitatively demonstrate the relative importance of the advective

flow of P into the porewater zone due to transpiration. For this analysis, we halved the leaf area index associated with each cell's macrophyte biomass (mimicking less dense canopy cover) for a 1980 test run compared to a 1980 nominal run. We used 1980 because it was a period when the region was continuously flooded (mean depth of 0.7 m), without large differences in plant biomass between runs. Table 1 shows that in the central sawgrass region (site U3, total biomass approximately 250 g C m^{-2}), average total ET was approximately the same for both the nominal- and reduced-canopy runs. In the northern cattail region (F1, total biomass approximately 1000 g C m^{-2}), total ET in the reduced-canopy condition was similar to that of the sawgrass site under both conditions (3.5 - 3.6 mm d^{-1}), but the denser canopy, nominal-condition at this site had somewhat higher ET (4.1 mm d^{-1}) than all others.

The principal differences emerged when we examined the relative contributions of transpiration vs. surface water evaporation. Transpiration increased consistently with increasing macrophyte canopy cover, (from 0.1 to 2.7 mm d^{-1}), while surface water evaporation decreased with less radiation reaching the water surface. With the higher transpiration and its advection of surface waters into the porewater, the conservative tracer concentration at least doubled at both the sawgrass and cattail sites. In terms of hydrologic exchange due to transpiration and downward advection, the time required for the upper 30 cm of the soil porewater to be completely replaced was as little as 3 months in the cattail site and several years in the reduced-canopy condition at the sawgrass site. Thus, depending on the concentration of P in the surface water relative to porewater and sorbed concentrations in the soil, this transport mechanism can potentially be a significant source of phosphorus to the plant root zone.

Model Results: Scenarios

The present-day WCA-2A eutrophication gradient includes noticeable changes in surface water and sediment phosphorus, macrophyte and periphyton biomass, and community types. What may have occurred if the nutrient loads had been significantly reduced in the early 1980's when eutrophication impacts were apparent in WCA-2A? For a hypothetical scenario, we curtailed the simulation's (1980-96) inorganic P inflow concentrations to a maximum of 6.0 μg L^{-1}, (compared to the observed mean of 62 μg L^{-1}).

Average differences between the nominal and reduced-load runs across the whole region were generally not large (Table 2). The expanse of marsh that is unimpacted by external phosphorus loads under either scenario heavily weights the regional mean values. However, subregions near the water control structure inflows were substantially affected by reduced loads.

While mean surface water P concentration for the entire region was 6 μg L^{-1} greater in the nominal run, more than 40% of the region had >20 μg L^{-1} higher P concentration compared to the reduced-load scenario in 1996. The periphyton response to the reduced P load was not apparent when viewing the regional mean difference (Table 2), but spatial differences were pronounced as discerned from maps of calcareous periphyton biomass. A mean difference map (Figure 14a) indicated a region of much higher biomass under the reduced-load scenario in the region immediately downstream of the S-10 A-E structures. The noncalcareous periphyton assemblage, while generally at a lower biomass in the region, tended to reflect an opposing trend (Figure 14b), but differences between runs were restricted to the area immediately downstream of the S-10 structures. These responses were primarily due to significantly reduced surface water nutrient concentrations in that region (Figure 15a), as there was little difference in shading from macrophyte biomass in the immediate vicinity of the S-10 structures (Figure 14c).

Simulation of soil nutrients produced a similar trend of more pronounced localized differences compared to region-wide changes under reduced-inflow loads. While region-wide mean P concentrations in the porewater and sorbed to the substrate were somewhat higher in the nominal compared to the reduced-load run (Table 2), the largest changes were observed in the current-day impacted zone near the S-10 structures. At site F1 near the inflow source, sorbed phosphorus was reduced 20% by 1996 under reduced external loads. Figure 15b shows that even in that reduced-load condition, the area continued to increase in concentration for approximately the first decade, after which the concentrations stopped their gradual increase. Porewater P concentrations were reduced by half at the end of the 17 yr simulation under reduced-load conditions at the F1 and F2 sites (Figure 15c). Sites farther downstream of the S-10 structures had smaller differences, with no apparent effect at the unimpacted U3 site 10 km downstream.

While this scenario analysis indicated that the magnitude and spatial extent of an elevated nutrient “front” was reduced with decreased loads, the simulated macrophyte biomass response was less pronounced in what is currently the impacted region. Under both scenarios, biomass of *Cladium* and *Typha* were near their maximum within the first ~4 km south of the S-10 A-D structures (e.g., south to F2), with little difference between the two scenarios in that particular subregion (Figure 14c). Differences on the order of 500 - 800 g C m^{-2} higher total biomass under the nominal vs. reduced load runs were evident in parts of the northwest region and the ridge/slough areas further south of the S-10 A-D structures. Reduced inflows also shifted macrophyte community types. There was a 33 km^2 reduction of the sawgrass/cattail mixture category and a 14 km^2 cover reduction of the pure cattail category in the reduced-load scenario compared to the nominal run.

Discussion

Spatial and temporal characteristics of the Everglades are well-described for some ecological processes, but there remain gaps in our quantitative understanding of all of the system's dynamics. For example, whereas some of the graminoid plant communities are reasonably well quantified with respect to standing biomass and tissue nutrient stoichiometry (Toth 1987, Toth 1988, Davis 1991, Miao and Sklar *in press*), changes in these characteristics are less well known across time and space for all species. In particular, the interaction of multiple factors (such as hydroperiod, nutrient availability, and fire regime) that are driving the changes in plant stock are not well understood, but relatively recent studies are providing better insight (Urban et al. 1993, Newman et al. 1996). Similarly, only recently have fine-scaled data been available on some of the processes behind changes in periphyton communities.

Hydrology drives the Everglades, and hydrology was a priority in our modeling and data compilation efforts. Because a hydrology model exists (MacVicar et al. 1984, HSM 1997), a reasonably detailed understanding of the system hydrology was available. However, a significant effort remained to obtain the relevant data for the purposes of our model that is of a different spatial scale and areal extent, and which also incorporates dynamic feedbacks among hydrology and plant biology. Water losses through evapotranspiration and friction effects of vegetation on overland flow are two very sensitive and important processes in determining regional and/or local water budgets. While macrophyte biomass dynamics over short time scales and limited areas may not significantly influence the total water budget for a region as large as WCA-2A, there is evidence (e.g., Table 1) that altered evapotranspiration associated with plant biomass and community shifts has the potential to alter water storages within particular locations. The linkages among hydrology, biogeochemistry, and plant biology can alter other ecosystem characteristics involving nutrient budgets and plant biomass (Figure 13 and Table 1).

Despite uncertainties associated with fully characterizing all of the dynamics of the complex Everglades system, we were able to calibrate and verify the CALM at a number of levels. The most rudimentary level of determining the extent to which a model is capturing reality is what we term a Level 1 calibration, where the model behavior is judged to exhibit "reasonable" behavior. Level 1 calibration for the CALM did not indicate any variable performance that was inconsistent with ecological principles or observations. Most of our calibration was at the intermediate Level 2, where we had useful spatial and temporal resolution, but which was only complete enough to characterize the system variables over subsets of the entire spatial and temporal domains. We demonstrated the extent to which simulated hydrologic and ecological variations in space and time were consistent with observed data (Figures 8 - 12).

Presentation of a formal verification of model behavior is lacking for the current implementation of the CALM. However, the general model fit to observed water stages over widely varying conditions is an informal verification that the model's hydrologic behavior is accurate. (In actuality, the initial model calibration was conducted for the years 1980-84, and subsequent extension of that time domain provided an implicit verification which we do not present here). An ideal level of calibration and verification for the CALM would be to have spatially distributed measurements of all important state variables at temporal scales sufficient to capture the spatial and temporal heterogeneity of the system - one set for calibration and an independent set for verification. Due to the difficulty of making all of these measurements, and because many variables of interest (such as vegetation biomass and community type) have not been measured historically over the appropriate spatio-temporal scales, this Level 3 calibration/verification was not attained. Nevertheless, we achieved realistic results and obtained good levels of fit of model and observations. Thus, we believe that for significant changes in environmental forcings, the model will provide realistic behavior.

Ecological implications

One of the fundamental aspects of model development is recognizing the degree of process complexity needed for the stated objectives and goals. We have arrived at what we believe to be an appropriate level of process-detail after extensive data analyses and ad hoc unit model experiments to analyze the effects of aggregation according to the principles described by Rastetter et al. (1992). The CALM/ELM is designed to run at varying spatial scales and for widely varying habitat types and environmental conditions. For habitats as diverse as fresh marshes and upland forests, we have evaluated the degree of sensitivity of the parameter set (Fitz et al. 1995). Using a modular framework, we have a modeling tool that can easily be aggregated or disaggregated. For example, the model's simulation of organic material decomposition and remineralization of nutrients currently is controlled by several factors, including temperature, moisture and substrate quality. We implicitly incorporate the redox potential in the sediments using a simple water depth - aerobic zone relation and generalized rate parameters for aerobic and anaerobic environments. This appears to be adequate for our current objectives, but would require more detailed relationships for finer scale modeling of nutrient availability in different layers of the root zone.

After evaluating the ecosystem's properties and the model's structure and dynamics, there emerge some aspects of the model that we would like to improve. While we are able to simulate the eutrophication gradient associated with the inflows from the water management structures, additional realism could be incorporated by introducing and tracking total phosphorus, in addition to P, as input from the structures. Currently, we assume that biological processes in surface and

pore waters are driven by dissolved inorganic P, and the organic phosphorus contribution to the sediment is via periphyton and macrophyte detritus, but not by direct deposition of allochthonous organic phosphorus. In addition, it could be useful to implement variable C:P stoichiometry dynamics of the plant biomass. However, all of these processes in combination will significantly increase the model's complexity. Given the uncertainties associated with many of the process rates for these complex interactions, it is "uncertain" that there will be a relative benefit associated with better predictability or effectiveness (Costanza and Sklar 1985, Costanza and Maxwell 1994) for our objectives of evaluating ecosystem responses on a regional scale. We anticipate future efforts to evaluate how these changes could affect simulation results.

Simulation results must be interpreted in a realistic and conservative manner. In some instances, the CALM produced spatial output for some variables that did not match measured data. For example, the model overestimated porewater concentration at the most eutrophic site (F1) (Figure 10b), while it underestimated peat accretion (and P storage) at that site (Figure 10c). The C:P stoichiometry and homogenous soil profile are simplified compared to the real system dynamics. Therefore, there is some uncertainty in our estimates of the timing and magnitude of the propagation of the nutrient "front" along the gradient associated with the S-10 structures. Similarly, it is likely that there is some uncertainty in model estimates of the time that internal P loading will continue in the highly impacted areas. Nevertheless, the model captured realistic dynamics of a complex system across large temporal and spatial extents, allowing us to further investigate the potential relative changes to be expected under a variety of altered external forcing functions. It is apparent that parts of the WCA-2A ecosystem will continue in a eutrophic state for a significant time period after reducing external inputs, and some ecological indicators (such as macrophytes) point to some continued expansion of the zone of impact from external forcing functions. The utility of the CALM lies not in producing exact spatial results, but rather in evaluating the types of interactions that occur in the ecosystem that are difficult to predict *a priori*, and are not captured in models of either hydrology or surface water quality alone. An example is the result showing that internal cycling of nutrients within the soils can continue to impose a load on the ecosystem long after external sources of nutrient inputs are curtailed (Figure 15). Alterations in hydroperiod, such as those that may occur with new water management scenarios, can significantly alter the pattern and magnitude of this internal cycling.

The simulated difference in remineralization rates (Figure 13) was as much as 2.5-3 times greater in drier regions, contributing to internal loading of available phosphorus. Koch-Rose et al. (1994) found peak porewater SRP at eutrophic sites following a summer drydown with high temperatures, and data to indicate that P may be a limiting factor in microbially-mediated nutrient mineralization along the WCA-2A gradient. Following agricultural drainage of the northern

Everglades, soil elevations decreased dramatically due to subsidence and peat oxidation (Snyder and Davidson 1994). The CALM incorporates both these feedbacks of hydroperiod and nutrient availability on decomposition rates. The temporal and spatial extent of the interactions that lead to such processes is fundamental to a spatially explicit ecological model such as CALM. Capturing these dynamic interactions in simulations allows an evaluation of the potential for the system to self-organize and change.

It is difficult, if not impossible, to use just one or two variables to predict total ecosystem response to altered management scenarios, given the multitude of interactions that occur in the real ecosystem. Water levels alone do not fully characterize the ecosystem response. Water, nutrients, and plants are important to understanding the system structure and function. For example, vegetation biomass and community types may change over relatively long time scales. This affects transpiration, nutrient uptake, and detrital accumulation, further influencing the ecosystem through continued feedbacks among hydrology, geochemistry, and ecosystem structure. These aspects of the ecosystem are important to how it functions: with changes to surface water phosphorus loading, a component of the system such as periphyton is indirectly altered by macrophyte shading in addition to the direct effect of new surface water chemistry (Figure 14). The results of the model sensitivity and scenario analyses suitably demonstrate these inter-relationships, and provide an improved understanding of the ecological response to water management.

Restoration implications

Significant reductions in nutrient loads to WCA-2A are anticipated within the next decade. However, our results suggest that reductions in nutrient loads through the S-10 structures will not have the immediate and dramatic effects that many are hoping to observe within the currently impacted regions of WCA-2A. This may be relatively surprising to some since nutrient processing by wetlands can be relatively fast (ca. days). One might expect to see rapid restoration to impacted areas once nutrient loads are reduced. This does not occur in the CALM because some regions of these wetland soils have significant nutrient storage which maintains the system in its present state, and can potentially continue to accumulate available nutrients, while at the same time spreading out spatially. Although surface water nutrients decline to low levels under reduced external load, the macrophyte biomass (and cattail areal coverage) associated with the currently impacted areas is not likely to decline in the near term. In fact, even after 17 years of reduced loads, the total plant biomass for much of the impacted zone remains similar to that under observed loads (Figure 14c). This indicates that another component of WCA-2A habitats, that of calcareous periphyton communities, will not likely undergo restoration in the near term because of light limitation under the dense vegetation canopy in the impacted zone.

There are a variety of tools, including models and other techniques, that will be used to aid in identifying optimal scenarios for improved water management in south Florida. In conjunction with boundary condition inputs from the SFWMM that simulates the entire system of water management, the ELM/CALM tools provide an ecological basis for evaluating indirect effects of altered water and nutrient flows as they propagate across the landscape mosaic of the Everglades wetlands. Without considering feedbacks among nutrient cycling/availability, hydrology, and plant community dynamics, simple predictions of the response to a change in one factor alone would be problematic. Changes in water delivery to the Water Conservation Areas can alter plant growth due to water limitation or excess. Different water levels also alter the decomposition rates of organic material in the soil, and thus affect the relative availability of nutrients. Thus, the interactions of plants and nutrient cycling could produce a different state of plant biomass and composition, one that was not expected from hydrologic considerations alone. The CALM has served as the testing platform for development of the larger ELM, which encompasses the entire "natural" area of the Everglades/Big Cypress system. Using a process-based landscape model to depict ecosystem dynamics in the Everglades will assist in developing more informed recommendations concerning management strategies. In this first version of a landscape modeling program for WCA-2A, we have demonstrated the nature of these ecosystem responses to a variety of environmental changes. We will continue to refine the model to incorporate new empirical studies, and are implementing the modeling framework within the entire Everglades system.

Acknowledgments

This work was initially supported by funding from the SFWMD (C-3123) to the University of Maryland, and continues to be supported at the SFWMD. R. Costanza was the Principal Investigator on the initial project, providing support and valuable input along the course of the work. A. Voinov was instrumental in developing and implementing many aspects of the hydrologic algorithms, particularly the raster-vector interaction modules. K. Rutchey and L. Vilchek were valuable contributors in many aspects of spatial characterization of WCA-2A, including the elevation data processing. P. McCormick and S. Newman kindly provided us with recent unpublished data from their field studies in WCA-2A, and on many occasions R. Reddy provided us with early results from his laboratory. Y. Wu and E. Reyes provided useful data summaries and advice during the development of the project. We would like to thank D. Worth and T. Fontaine for motivating and supporting the initiation of this project. Special thanks go to T. Maxwell for his Spatial Modeling Environment (http://kabir.cbl.umces.edu/SME3/) used in developing the CALM and ELM. We appreciate the thoughtful reviews of T. Fontaine, T. James, C. Madden, Z. Moustafa, and Y. Wu. Further descriptions of the model structure and

implementation, along with recent animations of model output, can be found at: http://sfwmd.gov/org/erd/esr/projects/ELM.html.

Literature cited

Bales, J. D., J. M. Fulford, and E. Swain. 1997. Review of selected features of the Natural Systems Model, and suggestions for application in South Florida. Report 97-4039. Water Resources Investigations, U.S. Geological Survey, Raleigh, NC.

Browder, J. A. 1982. Biomass and primary production of microphytes and macrophytes in periphyton habitats of the southern Everglades. South Florida Research Center. Homestead, FL. 49 pp.

Chen, Z., T. D. Fontaine, and R. Z. Xue. 1997. Phosphorus transport simulation in the Everglades Protection Area: a GIS-modeling approach. *In:* Proceedings of the 22nd Annual Conference of the National Association of Environmental Professionals, Orlando, FL.

Christiansen, J. E. 1968. Pan evaporation and evapotranspiration from climatic data. J. of Irrig. and Drain. Div. 94:243-265.

Cooper, R. M. and J. Roy. 1991. An atlas of surface water management basins in the Everglades: the Water Conservation Areas and Everglades National Park. South Florida Water Management District, West Palm Beach, FL. Sept. 1991.

Costanza, R. and T. Maxwell. 1994. Resolution and predictability: an approach to the scaling problem. Landscape Ecology. 9:47-57.

Costanza, R. and F. H. Sklar. 1985. Articulation, accuracy and effectiveness of mathematical models: a review of freshwater wetland applications. Ecological Modelling. 27:45-68.

Craft, C. B. and C. J. Richardson. 1993. Peat accretion and N, P, and organic C accumulation in nutrient-enriched and unenriched Everglades peatlands. Ecological Applications. 3(3):446-458.

Davis, J. H. 1943. The Natural Features of Southern Florida, Especially the Vegetation, and the Everglades. Florida Geological Survey, Tallahassee, FL.

Davis, S. M. 1982. Patterns of radiophosphorus accumulation in the Everglades after its introduction into suface water. Report 82-2. South Florida Water Management District, West Palm Beach, FL. February, 1982.

Davis, S. M. 1989. Sawgrass and cattail production in relation to nutrient supply in the Everglades. pp. 325-341*In:* Sharitz, R. R. and J. W. Gibbons (eds.). Freshwater Wetlands and Wildlife, DOE Symposium Series No. 61. USDOE Office of Scientific and Technical Information, Oak Ridge, Tennessee.

Davis, S. M. 1991. Growth, Decomposition and Nutrient Retention of *Cladium jamaicense* Crantz and *Typha domingensis* Pers. in the Florida Everglades. Aquatic Botany. 40:203-224.

DeBusk, W. F., K. R. Reddy, M. S. Koch, and Y. Wang. 1994. Spatial distribution of soil nutrients in a northern Everglades marsh - Water Conservation Area 2A. Soil Science Society of America Journal. 58(2):543-552.

Fennema, R. J., C. J. Neidrauer, R. A. Johnson, T. K. MacVicar, and W. A. Perkins. 1994. A computer model to simulate natural Everglades hydrology. pp. 249-290 *In* Davis, S. M. and J. C. Ogden (eds.). Everglades: the Ecosystem and its Restoration. St. Lucie Press, Delray Beach, FL.

Fitz, H. C., R. Costanza, and E. Reyes. 1993. The Everglades Landscape Model (ELM): Summary Report of Task 2, Model Development. Report to South Florida Water Management District, West Palm Beach, FL. 109 pp.

Fitz, H. C., E. B. DeBellevue, R. Costanza, R. Boumans, T. Maxwell, L. Wainger, and F. H. Sklar. 1996. Development of a general ecosystem model for a range of scales and ecosystems. Ecological Modelling. 88:263-295.

Fitz, H. C., A. Voinov, and R. Costanza. 1995. The Everglades Landscape Model: multiscale sensitivity analysis. Report to South Florida Water Management District, Everglades Systems Research Division. 88 pp.

HSM. 1997. Documentation update for the South Florida Water Management Model. Hydrologic Systems Modeling Division, South Florida Water Management District. West Palm Beach, FL. 239 pp.

Jensen, J. R., K. Rutchey, M. S. Koch, and S. Narumalani. 1995. Inland wetland change detection in the Everglades Water Conservation Area 2A using a time series of normalized remotely sensed data. Photogrammetric Engineering & Remote Sensing. 61:199-209.

Keith and Schnars. 1993. G.P.S. Geodetic Survey in the Everglades WCA-2A, and WCA-3A. Keith and Schnars, Lakeland Division, Lakeland, FL.

Koch, M. S. and K. R. Reddy. 1992. Distribution of soil and plant nutrients along a trophic gradient in the Florida Everglades. Soil Science Society of America Journal. 56(5):1492-1499.

Koch-Rose, M. S., K. R. Reddy, and J. P. Chanton. 1994. Factors controlling seasonal nutrient profiles in a subtropical peatland of the Florida Everglades. J Environ Qual. 23(3):526-533.

Lassiter, R. 1975. Modeling dynamics of biological and chemical components of aquatic ecosystems. Report EPA-660/3-75-012. Southeast Environmental Research Laboratory, U.S. Environmental Protection Agency.

Light, S. S. and J. W. Dineen. 1994. Water control in the Everglades: a historical perspective. pp. 47-84 *In* Davis, S. M. and J. C. Ogden (eds.). Everglades: The Ecosystem and its Restoration. St. Lucie Press, Delray Beach, FL.

MacVicar, T. K., T. VanLent, and A. Castro. 1984. South Florida Water Management Model: documentation report. Report 84-3. South Florida Water Management District. West Palm Beach, FL. December, 1983.

Maxwell, T. and R. Costanza. 1995. Distributed modular spatial ecosystem modelling. International Journal of Computer Simulation: Special Issue on Advanced Simulation Methodologies. 5(3):247-262.

McCormick, P. V. *pers. comm.* South Florida Water Management District, West Palm Beach, FL.

McCormick, P. V. and M. B. O'Dell. *in press.* Quantifying periphyton responses to phosphorus in the Florida Everglades: a synoptic-experimental approach. Journal of the North American Benthological Society.

McCormick, P. V., P. S. Rawlick, K. Lurding, E. P. Smith, and F. H. Sklar. *in press-a.* Periphyton-water quality relationships along a nutrient gradient in the Florida Everglades. Journal of the North American Benthological Society.

McCormick, P. V. and L. Scinto. 1998. Influence of phosphorus loading on periphyton communities in wetlands. p. ?? *In* Reddy, K. R. (ed.) Phosphorus Biogeochemistry in Sub-Tropical Ecosystems.

McCormick, P. V., R. B. E. Shuford, J. G. Backus, and W. C. Kennedy. *in press-b.* Spatial and seasonal patterns of periphyton biomass and productivity in the northern Everglades, Florida, USA. Hydrobiologia.

Meeder, J. F., M. S. Ross, G. J. Telesnicki, P. L. Ruiz, and J. P. Sah. 1996. Vegetation analysis in the C-111/Taylor Slough Basin. Report to the South Florida Water Management District. Southeast Environmental Research Program, Florida International University. Miami, FL.

Miao, S. L. and F. H. Sklar. *in press.* Biomass and nutrient allocation of sawgrass and cattail along a nutrient gradient in the Florida Everglades. Journal of Wetland Ecology and Management.

Newman, S. *pers. comm.* South Florida Water Management District, West Palm Beach, FL.

Newman, S., J. B. Grace, and J. W. Koebel. 1996. Effects of nutrients and hydroperiod on mixtures of *Typha*, *Cladium*, and *Eleocharis*: implications for Everglades restoration. Ecological Applications. 6:774-783.

Ogden, J. C., Robertson, W.B., G. E. Davis, and T. W. Schmidt. 1974. Pesticides, polychlorinated biphenyls and heavy metals in upper food chain levels, Everglades National Park and vicinity. U.S. Department of the Interior Report.

Rastetter, E. B., A. W. King, B. J. Cosby, G. M. Hornberger, R. V. O'Neill, and J. E. Hobbie. 1992. Aggregating fine-scale ecological knowledge to model coarser-scale attributes of ecosystems. Ecological Applications. 2:55-70.

Reddy, K., W. DeBusk, Y. Wang, D. R, and M. Koch. 1991. Physico-chemical properties of soils in the Water Conservation Area 2 of the Everglades. University of Florida. Gainesville, FL. 214 pp.

Reddy, K. R., R. D. Delaune, W. F. Debusk, and M. S. Koch. 1993. Long-term nutrient accumulation rates in the Everglades. Soil Science Society of America Journal. 57(4):1147-1155.

Richardson, C. J., C. B. Craft, R. G. Qualls, J. Stevenson, and P. Vaithiyanathan. 1995. Effects of Phosphorus and Hydroperiod Alterations on Ecosystem Structure and Function in the Everglades. Duke Wetland Center, Durham, NC. 371 p.

Richardson, C. J. and P. Vaithiyanathan. 1995. Phosphorus sorption characteristics of Everglades soils along a eutrophication gradient. Soil Science Society of America Journal. 59:1782-1788.

Rutchey, K. and L. Vilchek. 1992. Development of an Everglades vegetation map using a SPOT image and the global positioning system. Photogrammetric Engineering & Remote Sensing. 60:767-775.

Rutchey, K. and L. Vilchek. *submitted.* Air photo-interpretation and satellite imagery analysis techniques for mapping cattail coverage in a northern Everglades impoundment. Journal of Photogrammetric Engineering and Remote Sensing.

SFWMD. 1997. Proceedings of the Conference on: Atmospheric Deposition into South Florida: Measuring Net Atmospheric Inputs of Nutrients. South Florida Water Management District. West Palm Beach, FL.

Snyder, G. H. and J. M. Davidson. 1994. Everglades Agriculture - Past, Present, and Future. pp. 85-115 *In* Davis, S. M. and J. C. Ogden (eds.). Everglades: the Ecosystem and its Restoration. St. Lucie Press, Delray Beach, FL.

Swift, D. R. 1984. Periphyton and water quality relationships in the Everglades Water Conservation Areas. pp. 97-117 *In* Gleason, P. J. (ed.) Environments of South Florida: Present and Past. Miami Geological Society, Coral Gables, FL.

Swift, D. R. and R. B. Nicholas. 1987. Periphyton and water quality relationships in the Everglades Water Conservation Areas 1978-1982. Report 87-2. South Florida Water Management District, West Palm Beach, FL. March, 1987.

Toth, L. A. 1987. Effects of hydrologic regimes on lifetime production and nutrient dynamics of sawgrass. Report 87-6. South Florida Water Management District, West Palm Beach, FL.

Toth, L. A. 1988. Effects of hydrologic regimes on lifetime production and nutrient dynamics of cattail. Report 88-6. South Florida Water Management District, West Palm Beach, FL.

Urban, N. H., S. M. Davis, and N. G. Aumen. 1993. Fluctuations in sawgrass and cattail densities in Everglades Water Conservation Area 2A under varying nutrient, hydrologic and fire regimes. Aquatic Botany. 46:203-223.

Voinov, A., C. Fitz, and R. Costanza. *in press.* Surface water flow in landscape models: 1. Everglades case study. Ecological Modelling.

Voinov, A., H. C. Fitz, and R. Costanza. *submitted.* Everglades landscape hydrology: coupling raster and vector based models. Landscape Ecology.

Walker, W. W. 1998. Long term water quality trends in the Everglades. p. ?? *In* Reddy, K. R. (ed.) Phosphorus Biogeochemistry in Sub-Tropical Ecosystems.

Tables

Table 1. Transpiration and advection. Simulated response of year-1 (1980) mean total ET, surface water evaporation, and porewater transpiration to varying macrophyte canopy conditions. The Nominal condition used the nominal, best estimates of the leaf area index associated with the macrophytes at different sites (F1, U3) along the transect. The run under the Low Canopy condition used leaf area indices that were 0.5 x Nominal values. The final concentration of a conservative tracer determined the extent to which dissolved constituents were advected from the surface to the pore waters. Root zone turnover is the time required for transpiration and downward advection to completely replace the water volume in the upper 30 cm of soil of a continuously flooded area. (Actual root zone is 35 cm and 30 cm for sawgrass and cattail, respectively).

Variable	F1 Nominal	F1 Low Canopy	U3 Nominal	U3 Low Canopy
Total ET ($mm\ d^{-1}$)	4.1	3.6	3.6	3.5
Evaporation ($mm\ d^{-1}$)	1.4	2.5	3.0	3.4
Transpiration ($mm\ d^{-1}$)	2.7	1.1	0.6	0.2
Porewater tracer conc. ($\mu g\ L^{-1}$)	420	190	90	30
Root zone turnover (d)	89	218	400	1200

Table 2. Region-wide differences among scenarios. End-of-simulation (1996) summary of selected variables for the nominal vs. reduced-load (1980-1996) scenario. The Nominal run is the 12 month, WCA-wide mean of each variable. The Difference is the WCA-wide mean difference (nominal minus reduced load) for that year. The Minimum and Maximum differences are the cell-specific minimum and maximum differences for each variable during that year.

Variable	Units	Nominal	Difference	Minimum difference	Maximum difference
P surface water	$\mu g\ P\ L^{-1}$	6	6	-6	58
P porewater	$\mu g\ P\ L^{-1}$	109	28	-92	863
P sorbed	$mg\ P\ kg^{-1}$	12	3	-3	37
Periphyton - calcareous	$g\ C\ m^{-2}$	52	-0.1	-60	30
Periphyton - non-calcareous	$g\ C\ m^{-2}$	4	0.6	-8	57
Macrophytes	$g\ C\ m^{-2}$	520	240	-69	904

Figure Captions

Figure 1. The location and attributes of Water Conservation Area 2A in south Florida. Elevation (cm 1929 NGVD) indicates the presence of the major topographic gradients. Levees bound all sides of the impoundment, with the names of water control structures indicated around the periphery. Seven of the monitoring sites along a WCA-2A gradient transect are labeled F0-F5 and U3. Hydrologic monitoring gage 2-17 is adjacent to site U3.

Figure 2. Observed annual rainfall for WCA-2A. The simulation period encompasses 1980 - 1996, inclusive of extremely low and high rainfall years.

Figure 3. Observed annual sum of P (Mg = metric ton) flows through major water control structures of WCA-2A: a) inflows (S-7, S-10A, S-10C, S-10D), b) outflows (S-11A, S-11B, S-11C); and net flows for those structures ($\sum$inflow-$\sum$outflow). S-10E began operations in 1985.

Figure 4. The state variables and within-cell flows of the CALM's unit model, excluding hydrology which is also a component of the model dynamics (Figure 6). State variables are enclosed within rectangles in ALL_CAPS. Environmental forcing functions are in ovals. Phosphorus is in the form of dissolved P (DISS. P) in the surface water and soil porewater, P sorbed to soils (SORB. P), and incorporated in living and non-living organic carbon stocks. The latter include suspended organic matter in the surface water (SUSPENDED ORGANIC MAT.), organic matter accreted in soils (ACCRETED ORGANIC MATTER), photosynthetic (PHOTOBIO) and non-photosynthetic (NPHOTOBIO) components of macrophytes, standing dead detritus (STAND. DETRITUS), PERIPHYTON, and a generalized CONSUMER.

Figure 5. The spatial integration of a general unit model within the raster grid cell and canal/levee vector landscape. Each homogeneous cell in the modeled landscape is assigned a habitat type (shown here as Habitats 1-5), which is used to parameterize the model for that cell. Water and dissolved nutrients are fluxed spatially among grid cells and canal vectors. Within-cell dynamics and those spatial fluxes can alter the attributes (e.g., plant biomass, soil nutrient concentration) of the grid cells, including the habitat type.

Figure 6. Water storages and flows for the hydrologic module. The depths associated with water in surface, unsaturated, and saturated storages all vary dynamically.

Figure 7. Simulated annual hydroperiod for a relatively wet (1983) and dry (1989) year. The effect of the ridge and slough elevation pattern can be discerned in the central region, and the areas near the inflow structures and canals tend to have slightly longer hydroperiods than would

otherwise be the case. The monitoring sites along a WCA-2A gradient transect are indicated by unlabeled black circles.

Figure 8. Simulated and observed water stage at the 2-17 gage in the central region of WCA-2A (close to site U3 in Figure 1). The overall correlation coefficient (R^2) of the model fit to observed data is 0.70. There are a number of periods (e.g., 1986) for which we could not obtain observed data.

Figure 9. Simulated and observed concentration of P in the interstitial porewater in July 1990. The monitoring sites along a WCA-2A gradient transect are indicated by unlabeled black circles.

Figure 10. Simulated and observed data along a WCA-2A gradient transect. Site locations are shown in Figure 1. a) Porewater P concentration, comparing observed mean values from a 1.5 yr (1995-97) study with quarterly samples to the simulation means during that same period. b) Surface water P concentration, comparing observed mean values from a 3 yr (1994-96) study with biweekly samples to the corresponding 1994-96 simulation means. c) Simulated and observed mean annual peat accumulation rates, with the observed rates from Cesium-137 dating (1964-1990) of soil cores, and simulated rates are the mean rate during the 1980-1996 simulation. d) Total (photosynthetic and nonphotosynthetic) biomass of macrophytes. The observed data are the mean total biomass of a number of samples at each site in the 1994 spring/summer growing season, and the corresponding simulated data are total biomass for the corresponding cells in June 1994.

Figure 11. Simulated (sim) and observed (obs) transitions in habitat types in WCA-2A. The observed data from classified aerial photography were aggregated into the 0.25 km2 grid cell resolution of the CALM, and the simulation did not distinguish between the cattail and cattail dominant mix (90+% and 50+%) classifications used in the photograph classifications.

Figure 12. Mean values of selected variables over the 17-yr simulation, showing a) calcareous periphyton biomass, b) surface water P concentration, and c) macrophyte total (photosynthetic and nonphotosynthetic) biomass.

Figure 13. Annual mean difference between two 17-yr simulation runs. A test run with increased evapotranspiration was compared to the nominal run by subtracting the nominal from the test run values, plotting the differences for one dry year (1989). a) Depth of the zone of unsaturated water. b) Remineralization rate of P in the soil. c) Macrophyte total biomass.

Figure 14. Annual mean difference between two 17-yr simulation runs. A hypothetical scenario run with reduced P concentration in S-7 and S-10 inflows was compared to the nominal run by subtracting the nominal from the scenario run values, plotting the differences for the final

simulation year (1996). a) Calcareous periphyton biomass. b) Noncalcareous periphyton biomass. c) Macrophyte total biomass.

Figure 15. Simulated surface water and soil nutrient concentrations under the nominal condition of observed P loads and under the reduced-load condition. a) Surface water P concentration at the F1 (eutrophic) site. b) Sorbed P concentrations at the F1 site. c) Reduction, relative to the nominal simulation, in porewater P concentration with distance from the S-10 inflow structures.

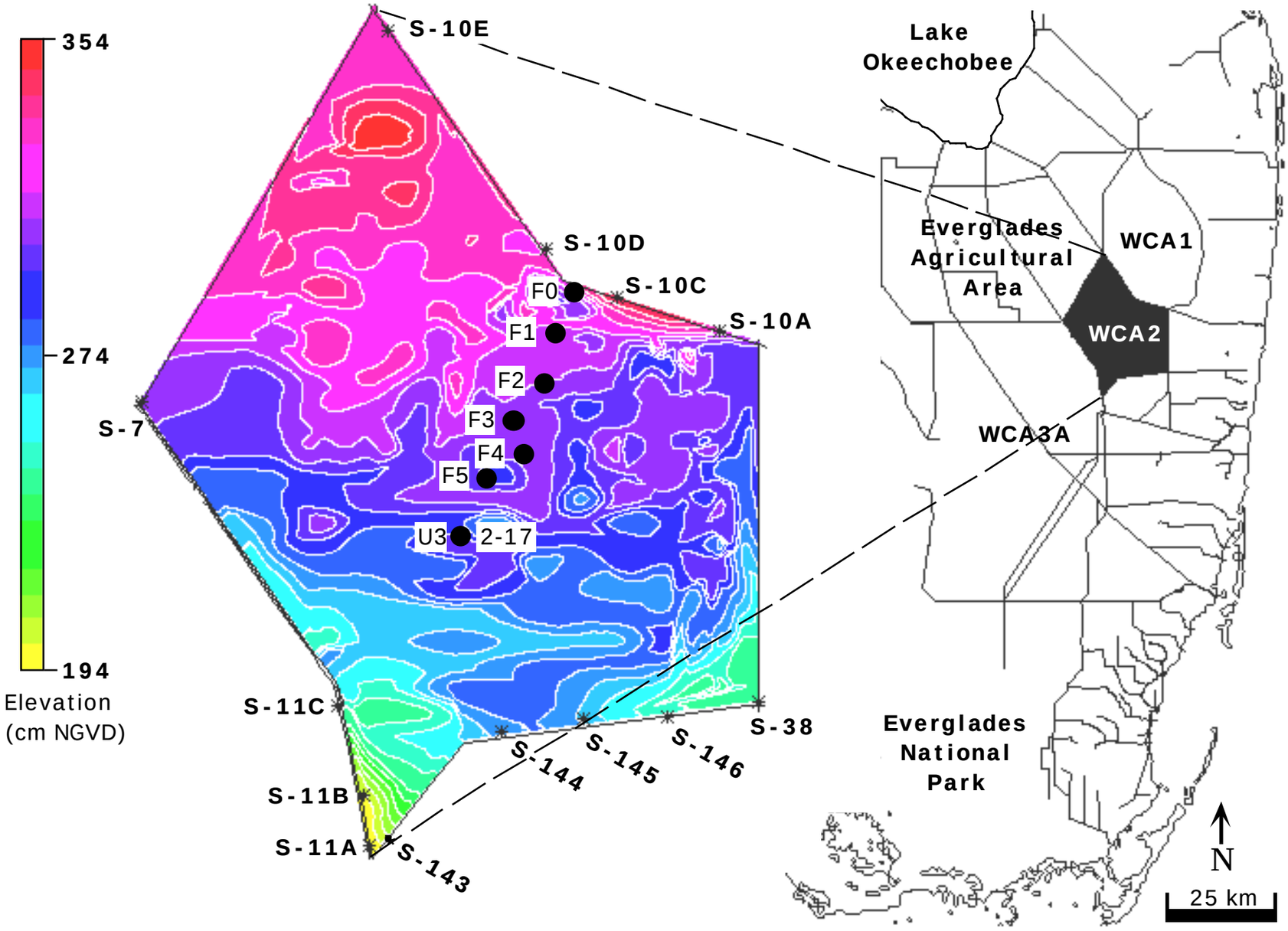
354
274
194
Elevation
(cm NGVD)
S-10E
S-10D
S-10C
S-10A
S-7
F0
F1
F2
F3
F4
F5
U3
2-17
S-11C
S-11B
S-11A
S-143
S-144
S-145
S-146
S-38
Lake
Okeechobee
Everglades
Agricultural
Area
WCA1
WCA2
WCA3A
Everglades
National
Park
N
25 km

Fig. 1

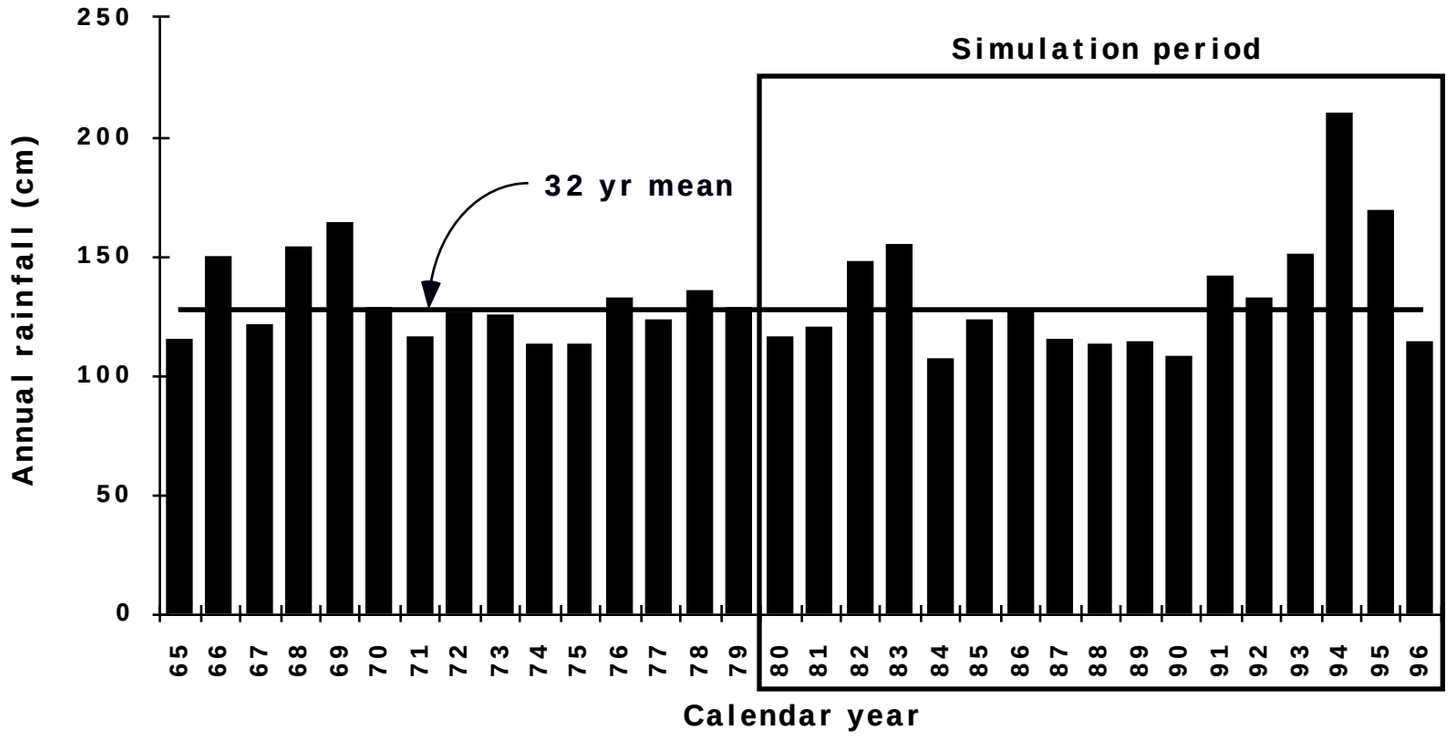
Simulation period
32 yr mean
Annual rainfall (cm)
250
200
150
100
50
0
65
66
67
68
69
70
71
72
73
74
75
76
77
78
79
80
81
82
83
84
85
86
87
88
89
90
91
92
93
94
95
96
Calendar year

Fig. 2

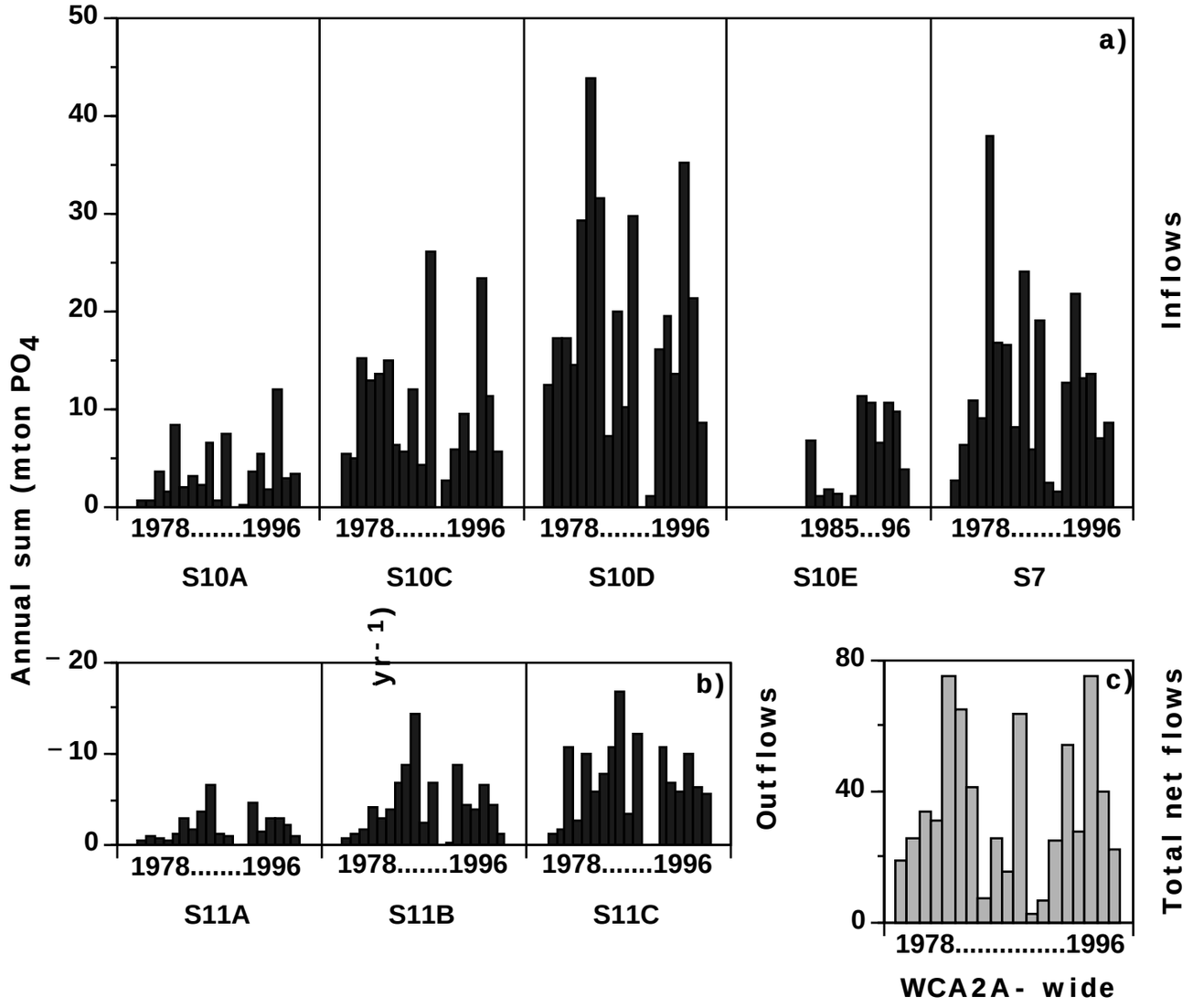
a)
Inflows
Annual sum (mton PO_4 yr^{-1})
50
40
30
20
10
0
1978.....1996
1985...96
S10A
S10C
S10D
S10E
S7
b)
Outflows
20
10
0
S11A
S11B
S11C
c)
Total net flows
80
40
0
WCA2A- wide

Fig. 3

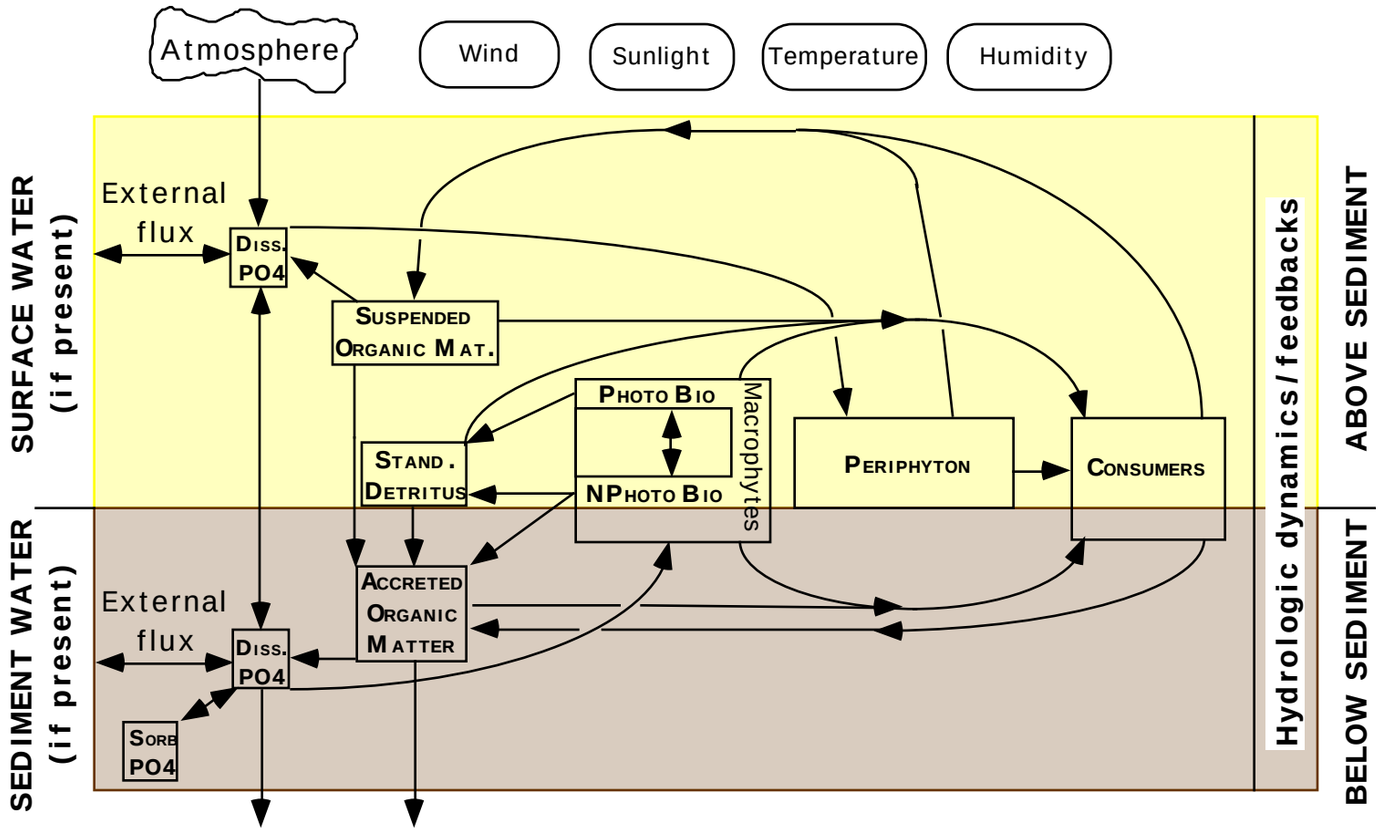
Atmosphere
Wind
Sunlight
Temperature
Humidity
SURFACE WATER (if present)
External flux
Diss. PO4
Suspended Organic Mat.
Photo Bio
NPhoto Bio
Macrophytes
Stand. Detritus
Periphyton
Consumers
Hydrologic dynamics/feedbacks
ABOVE SEDIMENT
BELOW SEDIMENT
SEDIMENT WATER (if present)
External flux
Accreted Organic Matter
Diss. PO4
Sorb PO4

Fig. 4

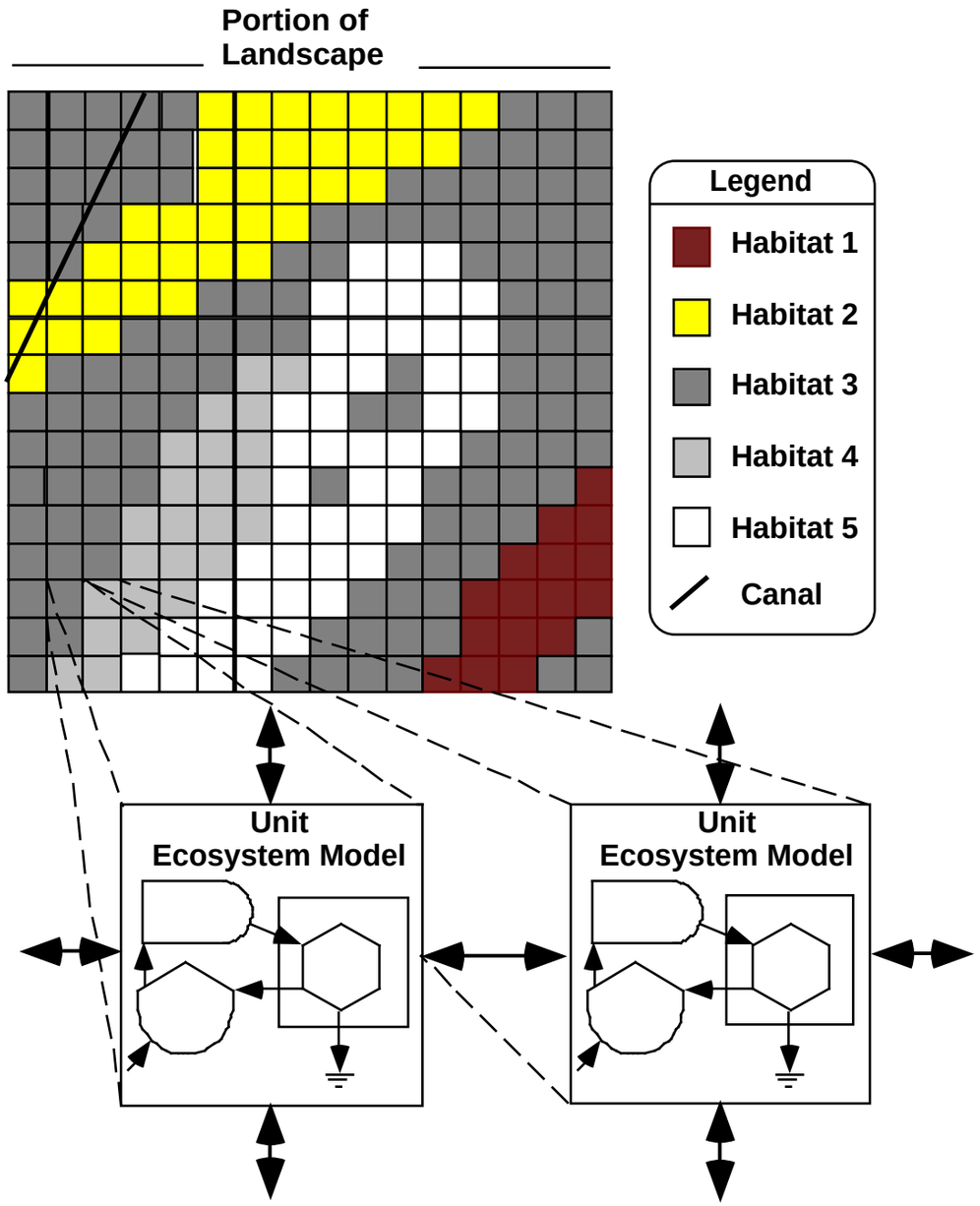
Portion of
Landscape
Legend
Habitat 1
Habitat 2
Habitat 3
Habitat 4
Habitat 5
Canal
Unit
Ecosystem Model
Unit
Ecosystem Model

Fig. 5

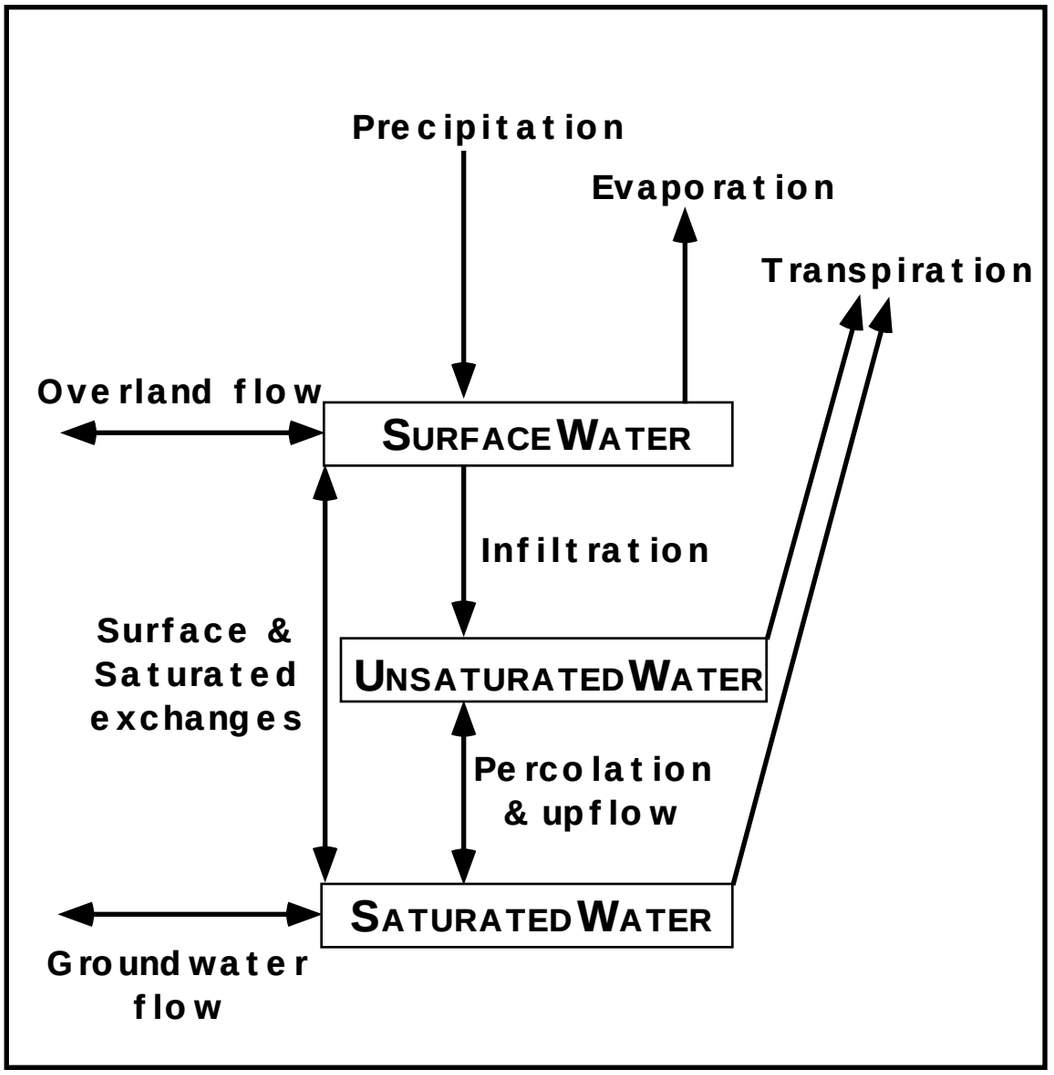
Precipitation
Evaporation
Transpiration
Overland flow
SURFACE WATER
Infiltration
Surface &
Saturated
exchanges
UNSATURATED WATER
Percolation
& upflow
SATURATED WATER
Groundwater
flow

Fig. 6

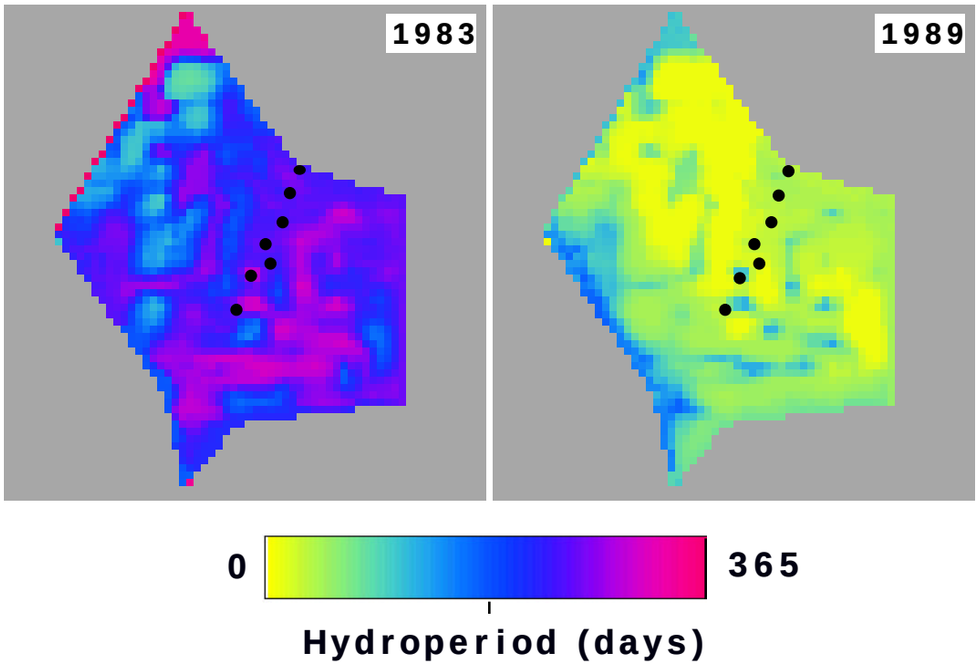

Fig. 7

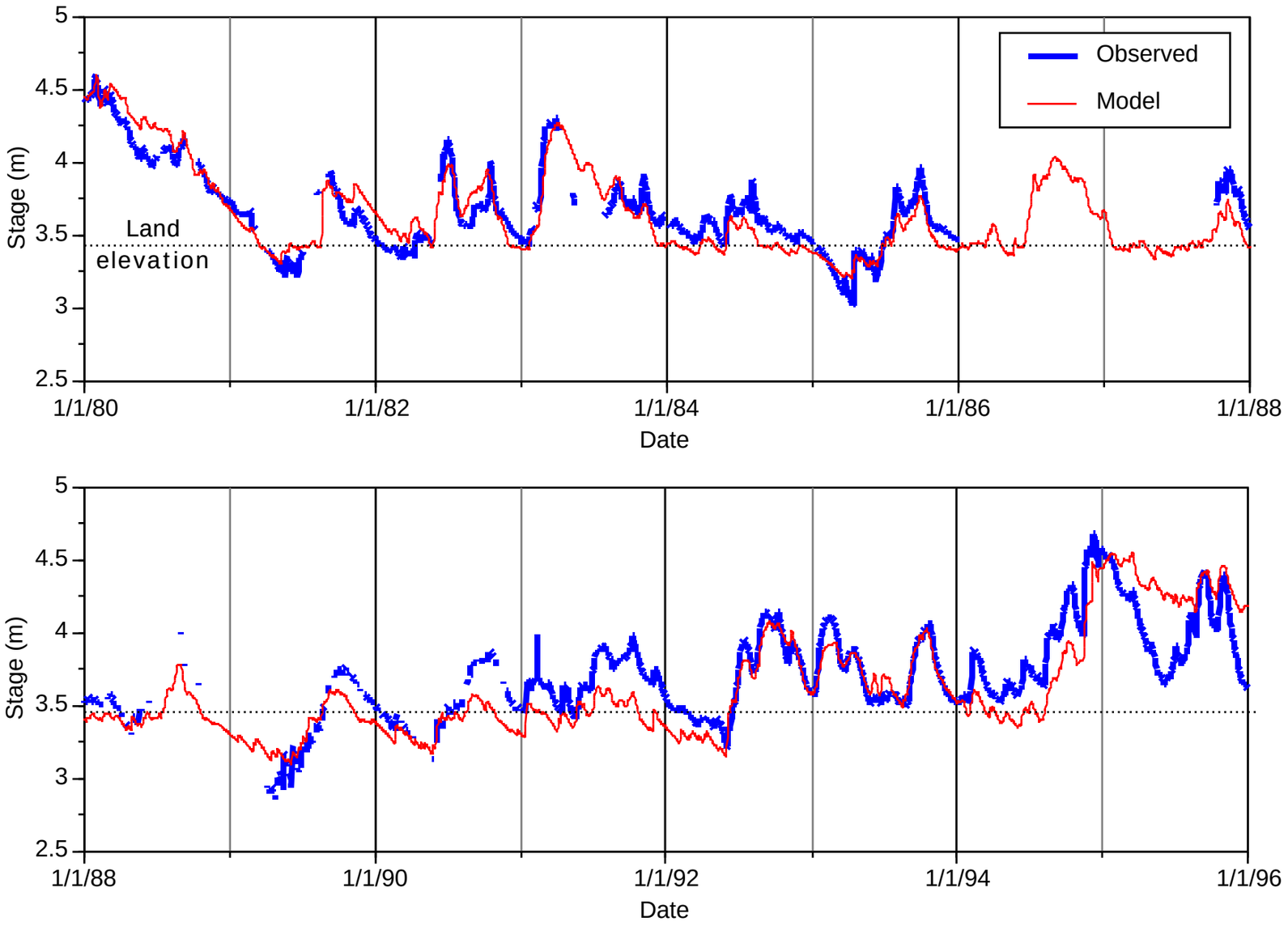
5
4.5
4
3.5
3
2.5
Stage (m)
Land
elevation
Observed
Model
1/1/80
1/1/82
1/1/84
1/1/86
1/1/88
Date

5
4.5
4
3.5
3
2.5
Stage (m)
1/1/88
1/1/90
1/1/92
1/1/94
1/1/96
Date

Fig. 8

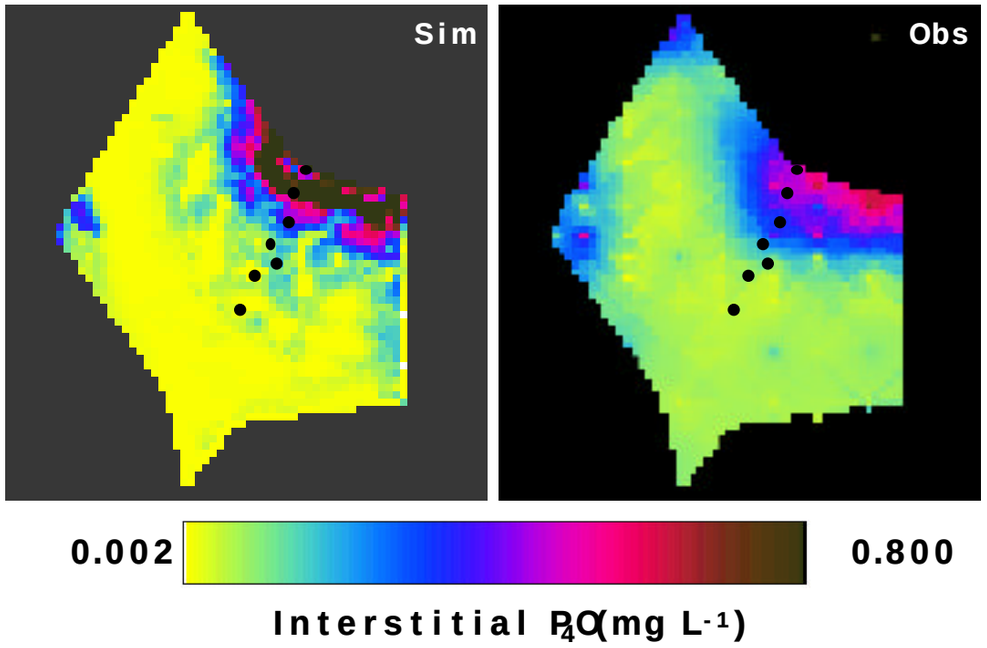

Fig. 9

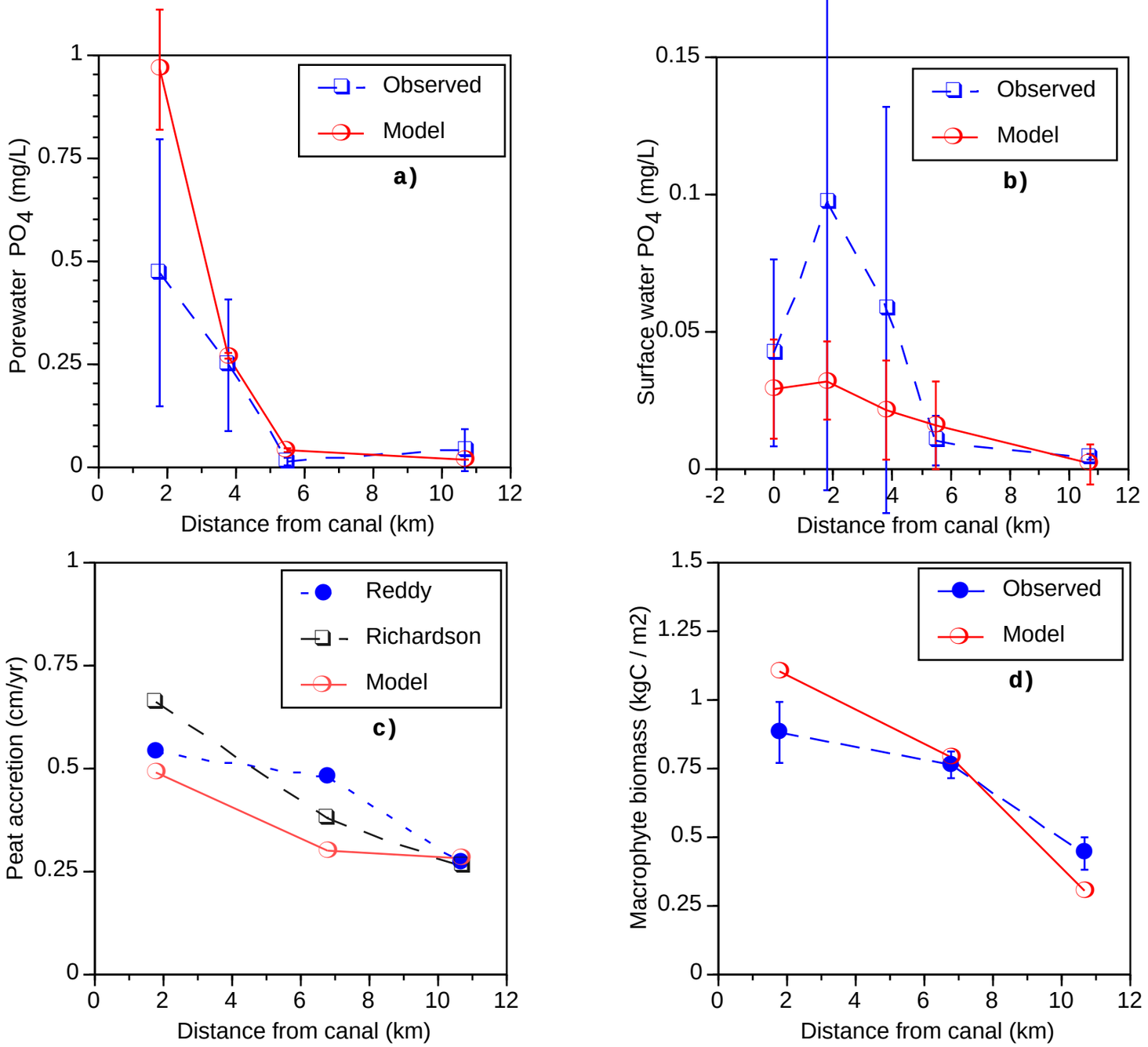
Porewater PO4 (mg/L)
Distance from canal (km)
Observed
Model
a)
Surface water PO4 (mg/L)
Distance from canal (km)
Observed
Model
b)
Peat accretion (cm/yr)
Distance from canal (km)
Reddy
Richardson
Model
c)
Macrophyte biomass (kgC / m2)
Distance from canal (km)
Observed
Model
d)

Fig. 10

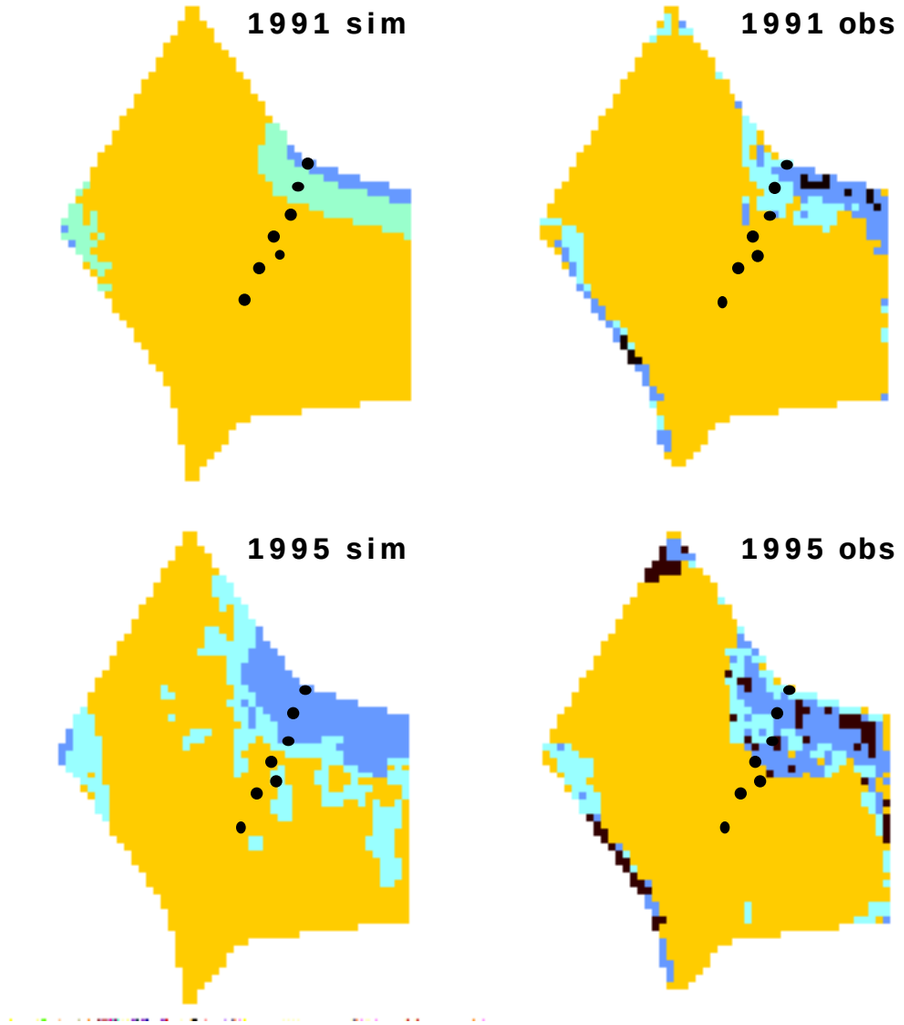

1991 (km^2) obs	1991 (km^2) sim	1995 (km^2) obs	1995 (km^2) sim	Classification	
4		18		Cattail 90+%	} lumped
24	8	41	49	Cattail 50+%	} for sim
25	36	36	68	Cattail 10+%	
380	389	337	316	Sawgrass etc.	

Fig. 11

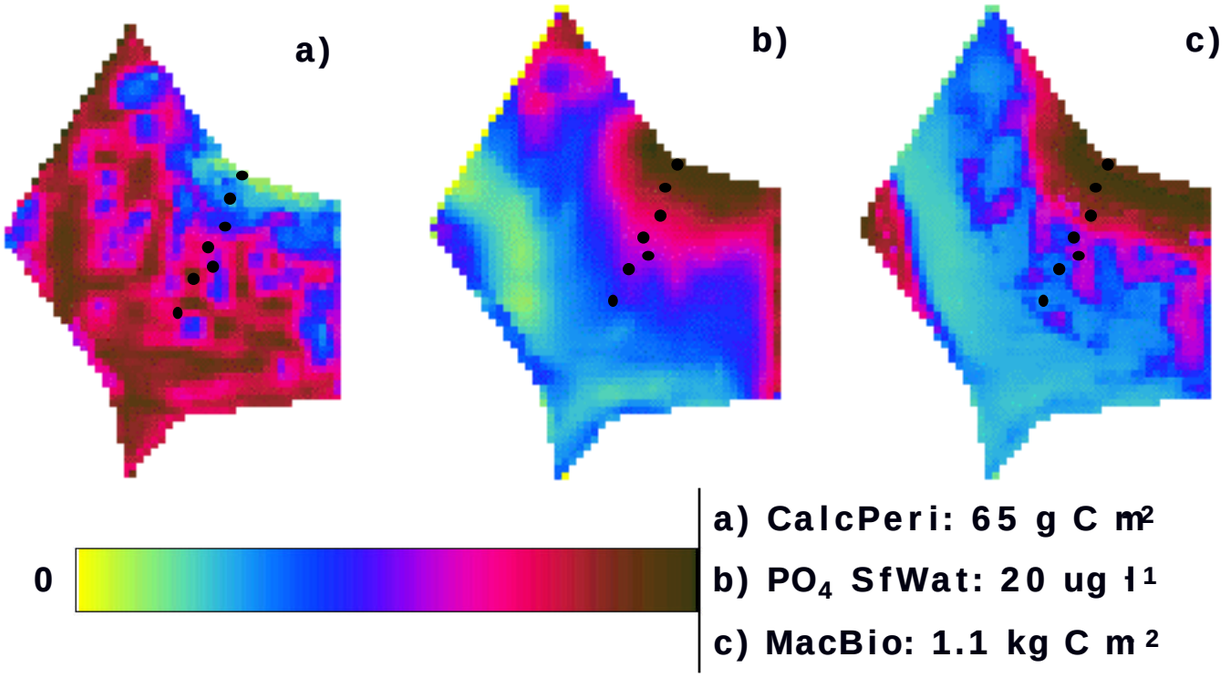

Fig. 12

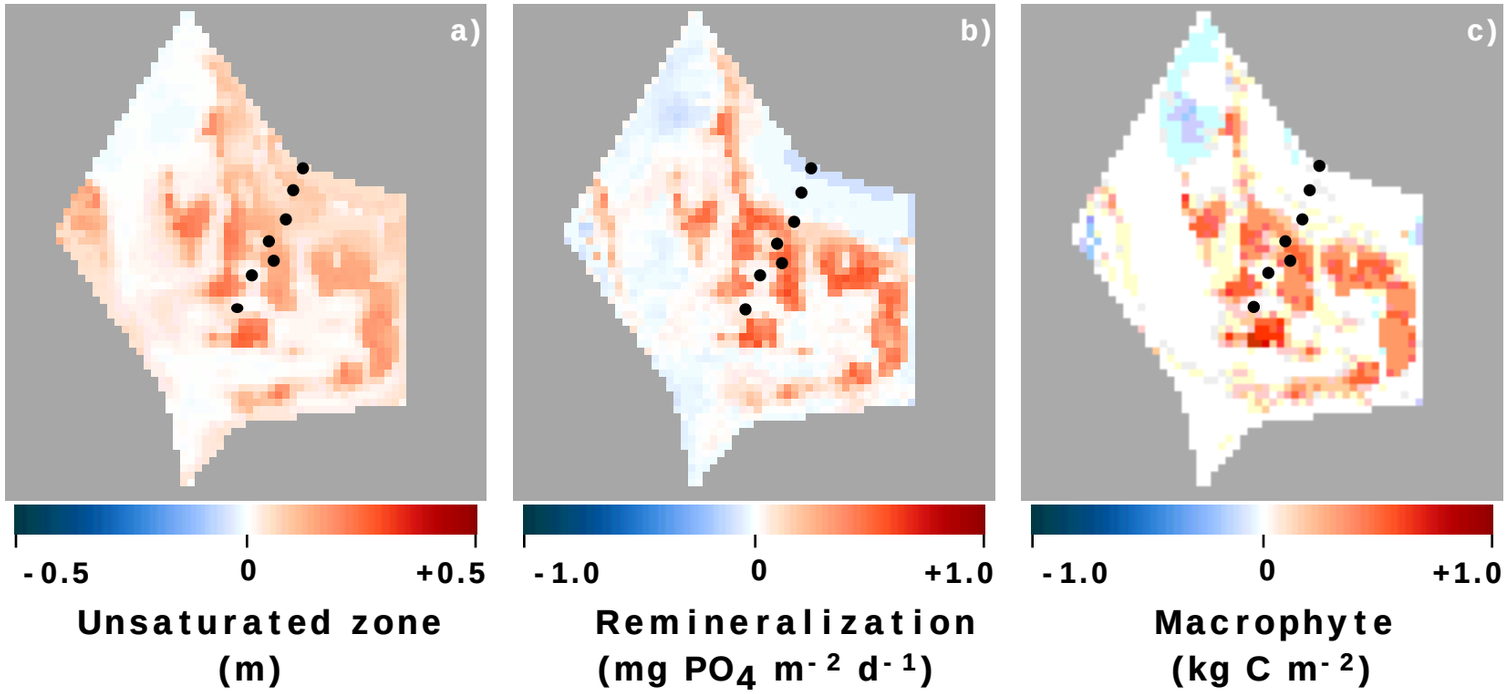
a)
b)
c)
-0.5
0
+0.5
-1.0
0
+1.0
-1.0
0
+1.0
Unsaturated zone
(m)
Remineralization
(mg PO4 m-2 d-1)
Macrophyte
(kg C m-2)

Fig. 13

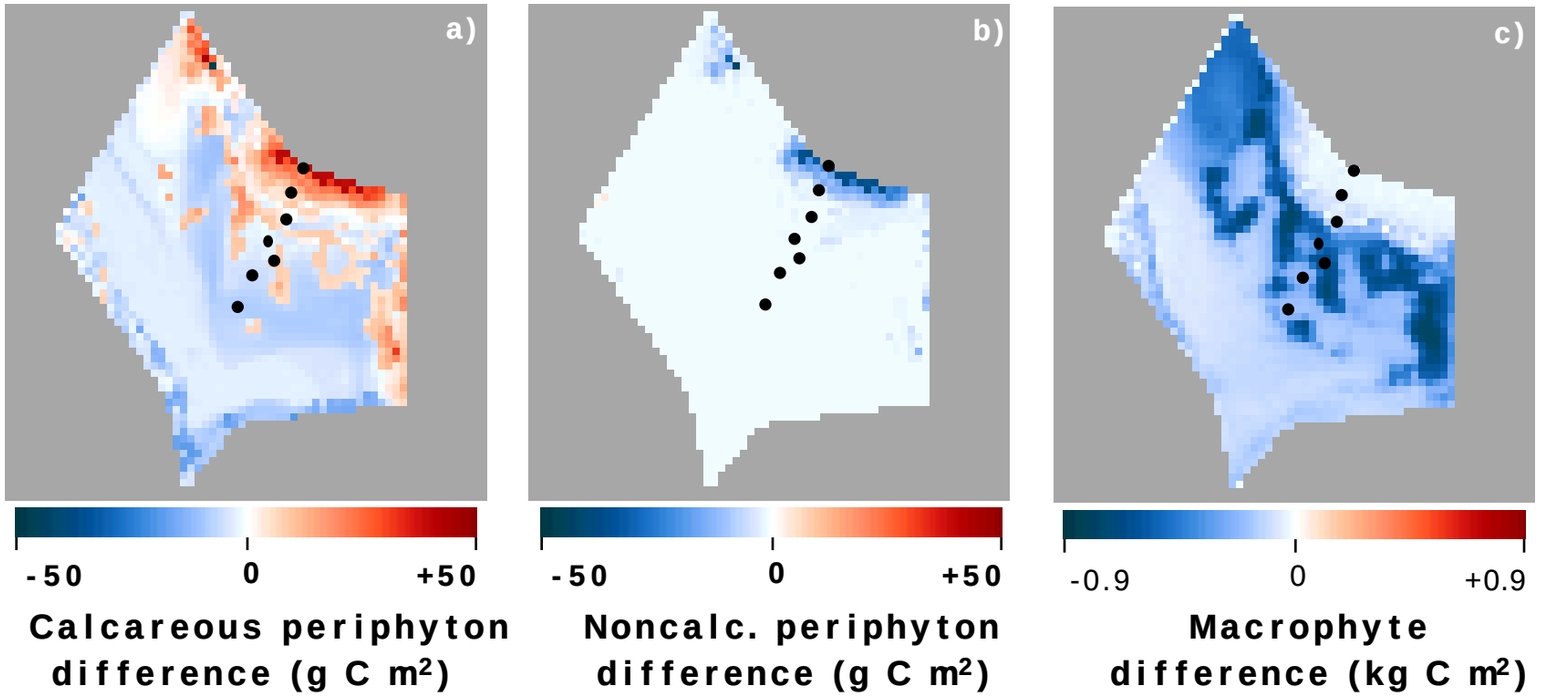
a)
b)
c)
-50
0
+50
-50
0
+50
-0.9
0
+0.9
Calcareous periphyton difference (g C m²)
Noncalc. periphyton difference (g C m²)
Macrophyte difference (kg C m²)

Fig. 14

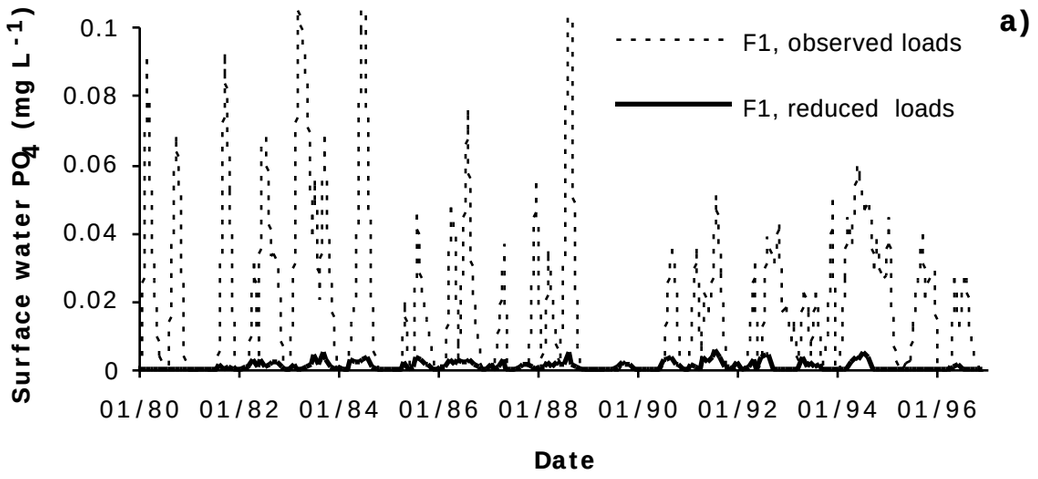
a)
F1, observed loads
F1, reduced loads
Surface water PO4 (mg L-1)
0.1
0.08
0.06
0.04
0.02
0
01/80 01/82 01/84 01/86 01/88 01/90 01/92 01/94 01/96
Date

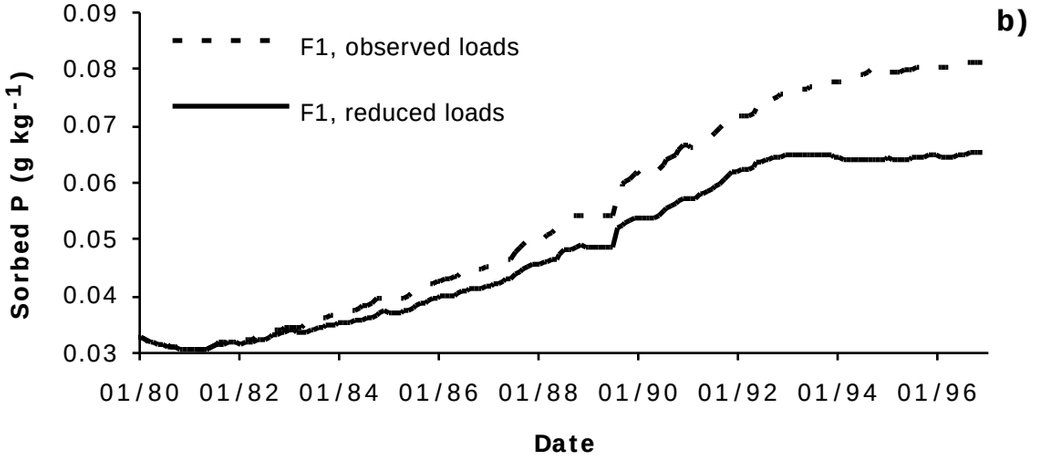
b)
F1, observed loads
F1, reduced loads
Sorbed P (g kg-1)
0.09
0.08
0.07
0.06
0.05
0.04
0.03
01/80 01/82 01/84 01/86 01/88 01/90 01/92 01/94 01/96
Date

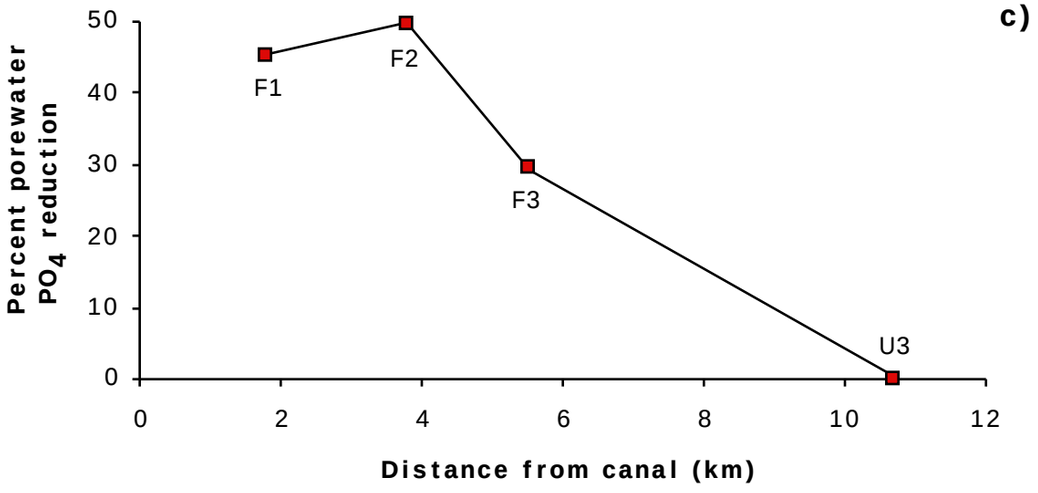
c)
Percent porewater PO4 reduction
50
40
30
20
10
0
F1
F2
F3
U3
0 2 4 6 8 10 12
Distance from canal (km)

Fig. 15